$\mu \to e\gamma$ and $\mu \to 3e$ processes with polarized muons and supersymmetric grand unified theories

Yasuhiro Okada*
Theory Group, KEK, Tsukuba, Ibaraki, 305-0801 Japan
and Department of Particle and Nuclear Physics, The Graduate University for Advanced Studies, Tsukuba, Ibaraki, 305-0801 Japan

Ken-ichi Okumura†
Theory Group, KEK, Tsukuba, Ibaraki, 305-0801 Japan
and Department of Accelerator Science, The Graduate University for Advanced Studies, Tsukuba, Ibaraki, 305-0801 Japan

Yasuhiro Shimizu‡
Theory Group, KEK, Tsukuba, Ibaraki, 305-0801 Japan
(Received 21 June 1999; published 14 March 2000)

$\mu^+ \to e^+\gamma$ and $\mu^+ \to e^+e^+e^-$ processes are analyzed in detail with polarized muons in supersymmetric grand unified theories. We first present a Dalitz plot distribution for $\mu^+ \to e^+e^+e^-$ decay based on an effective Lagrangian with general lepton-flavor-violating couplings and define various *P*- and *T*-odd asymmetries. We calculate branching ratios and asymmetries in supersymmetric SU(5) and SO(10) models taking into account complex soft supersymmetry breaking terms. Imposing constraints from experimental bounds on the electron, neutron, and atomic electric dipole moments, we find that the *T*-odd asymmetry for $\mu^+ \to e^+e^+e^-$ can be 15% in the SU(5) case. *P*-odd asymmetry with respect to muon polarization for $\mu^+ \to e^+\gamma$ varies from -100 to 100 % for the SO(10) model while it is $+100\%$ in the SU(5) case. We also show that the *P*-odd asymmetries in $\mu^+ \to e^+e^+e^-$ and the ratio of $\mu^+ \to e^+e^+e^-$ and $\mu^+ \to e^+\gamma$ branching fractions are useful to distinguish different models.

PACS number(s): 13.35.Bv, 11.30.Fs, 13.88.+e

I. INTRODUCTION

In order to explore physics beyond the standard model (SM), rare decay experiments can play a complementary role to the direct search for new particles at the high energy frontier. Through forbidden or very suppressed processes within the minimal SM, we may be able to obtain information on the interaction at the energy scale not accessible by collider experiments. The search for lepton flavor violation (LFV) is one of such windows to new physics.

In recent years, LFV processes have received much attention because in the supersymmetric (SUSY) grand unified theory (GUT) the branching ratios for $\mu^+ \to e^+\gamma$ and $\mu^+ \to e^+e^+e^-$ and the μ-e conversion rate in a nucleus can reach just below present experimental values [1–4]. The present experimental upper bounds of these LFV processes are $B(\mu^+ \to e^+\gamma) \leqslant 1.2 \times 10^{-11}$ [5], $B(\mu^+ \to e^+e^+e^-) \leqslant 1.0 \times 10^{-12}$ [6], and $\sigma(\mu^- \mathrm{Ti} \to e^- \mathrm{Ti})/\sigma(\mu^- \mathrm{Ti} \to \mathrm{capture}) \leqslant 6.1 \times 10^{-13}$ [7]. It is possible that future experiments will improve the sensitivity by two or three orders of magnitude below the current bounds [8,9].

In this paper we discuss the $\mu^+ \to e^+\gamma$ and $\mu^+ \to e^+e^+e^-$ processes in SUSY GUT. We focus on various asymmetries defined with the help of initial muon polarization. Experimentally, polarized positive muons are available by the surface muon method because muons emitted from π^+'s stopped at target surface are 100% polarized in the direction opposite to the muon momentum [10]. It is shown in Ref. [11] that the muon polarization is useful to suppress the background processes in the $\mu^+ \to e^+\gamma$ search. As for the signal distribution of $\mu^+ \to e^+\gamma$, the angular distribution with respect to the muon polarization can distinguish between $\mu^+ \to e_L^+\gamma$ and $\mu^+ \to e_R^+\gamma$. For $\mu^+ \to e^+e^+e^-$, distribution in the Dalitz plot and various asymmetries defined with help of the muon polarization carry information on chirality and Lorentz structure of LFV couplings. In particular, we can define *T*-odd asymmetry which is sensitive to *CP* violation in LFV interactions [12]. In the previous paper [13] we pointed out that sizable *T*-odd asymmetry can occur in the SU(5) SUSY GUT when a *CP* violating phase is introduced in one of the soft SUSY breaking parameters, i.e., the universal trilinear scalar coupling constant A_0. The purpose of this paper is to give a model-independent framework for analyzing the $\mu^+ \to e^+\gamma$ and $\mu^+ \to e^+e^+e^-$ processes and investigate specific features of the SU(5) and SO(10) SUSY GUT focusing on the *T*-odd and other asymmetries. Detailed comparison of the *T*-odd asymmetry with the electron, neutron and Hg electric dipole moments (EDM) is also done introducing SUSY *CP* violating phases within the minimal supergravity (SUGRA) model.

In Sec. II we describe effective Lagrangian of the processes $\mu^+ \to e^+\gamma$ and $\mu^+ \to e^+e^+e^-$. We introduce a *P*-odd asymmetry for $\mu^+ \to e^+\gamma$ and two types of *P*-odd asymmetries and a *T*-odd asymmetry for $\mu^+ \to e^+e^+e^-$. In Sec. III we introduce the SU(5) and SO(10) SUSY GUT and briefly review how LFV processes arise in these theories. In Sec. IV we present results of our numerical calculations. We calcu-

*Email address: yasuhiro.okada@kek.jp
†Email address: ken-ichi.okumura@kek.jp
‡Email address: yasuhiro.shimizu@kek.jp

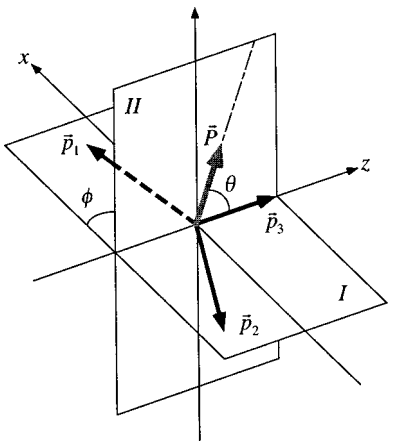

FIG. 1. Kinematics of the $\mu^+\to e^+e^+e^-$ decay in the center-of-mass system of muon. Plane I represents the decay plane on which the momentum vectors $\vec{p}_1$, $\vec{p}_2$, $\vec{p}_3$ lie, where $\vec{p}_1$ and $\vec{p}_2$ are momenta of two e^+'s and $\vec{p}_3$ is momentum of e^-, respectively. Plane II is the plane which the muon polarization vector $\vec{P}$ and $\vec{p}_3$ make.

late the branching ratios and the asymmetries in the SUSY SU(5) and SO(10) models taking into account complex soft SUSY breaking terms under the constraints imposed by the EDM experiments. We find that the *T*-odd asymmetry can be 15% in the SU(5) case while it is less than 0.01% in the SO(10) case. We also show that the *P*-odd asymmetry for $\mu^+\to e^+\gamma$ varies -100–$100\,\%$ for the SO(10) model and 100% for the SU(5) case. In the SU(5) case the *P*-odd asymmetries in $\mu^+\to e^+e^+e^-$ can reach $\pm 30\%$ and the ratio of $\mu^+\to e^+\gamma$ and $\mu^+\to e^+e^+e^-$ branching fractions varies over SUSY parameter space. On the contrary these asymmetries are smaller and the ratio of two branching fractions is almost constant in the SO(10) case. In appendices, useful formulas are listed.

II. PHENOMENOLOGY OF THE $\mu^+\to e^+\gamma$ AND $\mu^+\to e^+e^+e^-$ PROCESSES

We begin with the effective Lagrangian for $\mu^+\to e^+\gamma$ and $\mu^+\to e^+e^+e^-$ processes. Using the electromagnetic gauge invariance and the Fierz rearrangement we can write without loss of generality:

$$\begin{aligned}\mathcal{L}=&-\frac{4G_F}{\sqrt{2}}\{m_\mu A_R\bar{\mu}_R\sigma^{\mu\nu}e_L F_{\mu\nu}+m_\mu A_L\bar{\mu}_L\sigma^{\mu\nu}e_R F_{\mu\nu}\\&+g_1(\bar{\mu}_R e_L)(\bar{e}_R e_L)+g_2(\bar{\mu}_L e_R)(\bar{e}_L e_R)\\&+g_3(\bar{\mu}_R\gamma^\mu e_R)(\bar{e}_R\gamma_\mu e_R)+g_4(\bar{\mu}_L\gamma^\mu e_L)(\bar{e}_L\gamma_\mu e_L)\\&+g_5(\bar{\mu}_R\gamma^\mu e_R)(\bar{e}_L\gamma_\mu e_L)+g_6(\bar{\mu}_L\gamma^\mu e_L)(\bar{e}_R\gamma_\mu e_R)\\&+\text{H.c.}\},\end{aligned}\tag{1}$$

where G_F is the Fermi coupling constant and m_μ is the muon mass. The chirality projection is defined by the projection operators $P_R=(1+\gamma_5)/2$ and $P_L=(1-\gamma_5)/2$. $\sigma_{\mu\nu}$ is defined as $\sigma_{\mu\nu}=(i/2)[\gamma_\mu,\gamma_\nu]$. $A_L(A_R)$ is the dimensionless photon-penguin coupling constant which contributes to $\mu^+\to e_L^+\gamma$ ($\mu^+\to e_R^+\gamma$). These couplings also induce the $\mu^+\to e^+e^+e^-$ process. g_i's $(i=1-6)$ are dimensionless four-fermion coupling constants which only contribute to $\mu^+\to e^+e^+e^-$. g_1 and g_2 are scalar type coupling constants and g_i's $(i=3-6)$ are vector type coupling constants. $A_{L,R}$ and g_i's $(i=1-6)$ are generally complex numbers and calculated based on a particular model with LFV interactions.

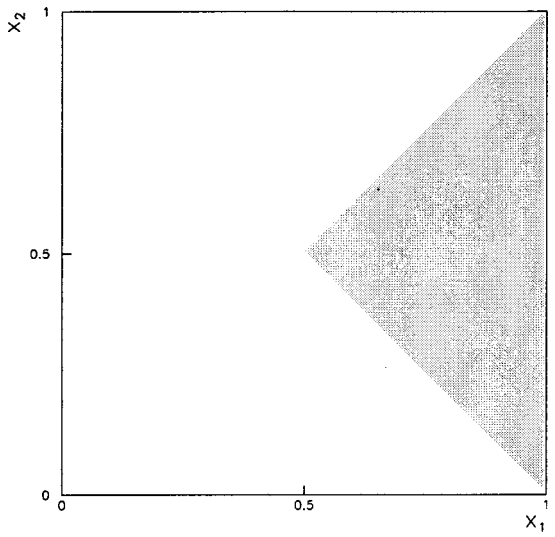

FIG. 2. Kinematical region of the $\mu^+\to e^+e^+e^-$ decay in the center-of-mass system of muon. x_1 (x_2) represents a larger (smaller) energy of decay positrons normalized by $m_\mu/2$. A light shaded region is allowed.

The differential branching ratio for $\mu^+\to e^+\gamma$ is given by

$$\begin{aligned}\frac{dB(\mu^+\to e^+\gamma)}{d\cos\theta}&=192\pi^2\{|A_L|^2(1+P\cos\theta)\\&\quad+|A_R|^2(1-P\cos\theta)\}\end{aligned}\tag{2}$$

$$\begin{aligned}&=\frac{B(\mu^+\to e^+\gamma)}{2}\{1+A(\mu^+\to e^+\gamma)\\&\quad\times P\cos\theta\},\end{aligned}\tag{3}$$

where the total branching ratio for $\mu^+\to e^+\gamma$ $[B(\mu^+\to e^+\gamma)]$ and the *P*-odd asymmetry $[A(\mu^+\to e^+\gamma)]$ are defined as

$$B(\mu^+\to e^+\gamma)=384\pi^2(|A_L|^2+|A_R|^2),\tag{4}$$

$$A(\mu^+\to e^+\gamma)=\frac{|A_L|^2-|A_R|^2}{|A_L|^2+|A_R|^2}.\tag{5}$$

Here P is the muon polarization and θ is the angle between the positron momentum and the polarization direction.

Kinematics of the $\mu^+\to e^+e^+e^-$ process with a polarized muon is determined by two energy variables of decay positrons and two angle variables which indicate the direction of the muon polarization with respect to the decay plane. In Fig. 1 we take the z axis as the direction of the decay electron

momentum ($\vec{p}_3$) and the z-x plane as the decay plane. Polar angles (θ,φ) $(0\leqslant\theta\leqslant\pi, 0\leqslant\varphi<2\pi)$ indicate the direction of the muon polarization $\vec{P}$. We take a convention that the decay positron having larger energy is named positron 1 and the other is positron 2 and $(p_1)_x \geqslant 0$. We define the energy variables as $x_1=2E_1/m_\mu$ and $x_2=2E_2/m_\mu$ where E_1 and E_2 are the energy of the positron 1 and 2, respectively. In this convention (x_1,x_2) represents one point of the Dalitz plot (Fig. 2). In our calculation we neglect the electron mass compared to the muon mass except for the total branching ratio. In order to avoid logarithmic singularity we have to take into account the electron mass properly to evaluate the total branching ratio.

Using the coupling constants in the Lagrangian in Eq. (1) the differential branching ratio for $\mu^+ \to e^+e^+e^-$ is written as follows:

$$\begin{aligned}\frac{dB}{dx_1dx_2d\cos\theta d\varphi}=\frac{3}{2\pi}[&C_1\alpha_1(x_1,x_2)(1+P\cos\theta)+C_2\alpha_1(x_1,x_2)(1-P\cos\theta)\\&+C_3\{\alpha_2(x_1,x_2)+P\beta_1(x_1,x_2)\cos\theta+P\gamma_1(x_1,x_2)\sin\theta\cos\varphi\}\\&+C_4\{\alpha_2(x_1,x_2)-P\beta_1(x_1,x_2)\cos\theta-P\gamma_1(x_1,x_2)\sin\theta\cos\varphi\}\\&+C_5\{\alpha_3(x_1,x_2)+P\beta_2(x_1,x_2)\cos\theta+P\gamma_2(x_1,x_2)\sin\theta\cos\varphi\}\\&+C_6\{\alpha_3(x_1,x_2)-P\beta_2(x_1,x_2)\cos\theta-P\gamma_2(x_1,x_2)\sin\theta\cos\varphi\}\\&+C_7\{\alpha_4(x_1,x_2)(1-P\cos\theta)+P\gamma_3(x_1,x_2)\sin\theta\cos\varphi\}\\&+C_8\{\alpha_4(x_1,x_2)(1+P\cos\theta)-P\gamma_3(x_1,x_2)\sin\theta\cos\varphi\}\\&+C_9\{\alpha_5(x_1,x_2)(1+P\cos\theta)-P\gamma_4(x_1,x_2)\sin\theta\cos\varphi\}\\&+C_{10}\{\alpha_5(x_1,x_2)(1-P\cos\theta)+P\gamma_4(x_1,x_2)\sin\theta\cos\varphi\}\\&+C_{11}P\gamma_3(x_1,x_2)\sin\theta\sin\varphi-C_{12}P\gamma_4(x_1,x_2)\sin\theta\sin\varphi],\end{aligned} \tag{6}$$

where C_i are expressed by the coupling constants g_i $(i=1-6)$ and $A_{L,R}$ as

$$C_1=\frac{|g_1|^2}{16}+|g_3|^2,\quad C_2=\frac{|g_2|^2}{16}+|g_4|^2,$$

$$C_3=|g_5|^2,\quad C_4=|g_6|^2,\quad C_5=|eA_R|^2,\quad C_6=|eA_L|^2,$$

$$C_7=Re(eA_Rg_4^*),\quad C_8=Re(eA_Lg_3^*),\quad C_9=Re(eA_Rg_6^*),\quad C_{10}=Re(eA_Lg_5^*),$$

$$C_{11}=Im(eA_Rg_4^*+eA_Lg_3^*),\quad C_{12}=Im(eA_Rg_6^*+eA_Lg_5^*), \tag{7}$$

where $e(>0)$ is the positron charge and P is the magnitude of the polarization vector. Functions α_i, β_i, and γ_i are defined as

$$\alpha_1(x_1,x_2)=8(2-x_1-x_2)(x_1+x_2-1), \tag{8}$$

$$\alpha_2(x_1,x_2)=2\{x_1(1-x_1)+x_2(1-x_2)\}, \tag{9}$$

$$\alpha_3(x_1,x_2)=8\left\{\frac{2x_2^2-2x_2+1}{1-x_1}+\frac{2x_1^2-2x_1+1}{1-x_2}\right\}, \tag{10}$$

$$\alpha_4(x_1,x_2)=32(x_1+x_2-1), \tag{11}$$

$$\alpha_5(x_1,x_2)=8(2-x_1-x_2), \tag{12}$$

$$\beta_1(x_1,x_2)=2\frac{(x_1+x_2)(x_1^2+x_2^2)-3(x_1+x_2)^2+6(x_1+x_2)-4}{(2-x_1-x_2)}, \tag{13}$$

$$\beta_2(x_1,x_2)=\frac{8}{(1-x_1)(1-x_2)(2-x_1-x_2)}\times\{2(x_1+x_2)(x_1^3+x_2^3)-4(x_1+x_2)$$
$$\times(2x_1^2+x_1x_2+2x_2^2)+(19x_1^2+30x_1x_2+19x_2^2)-12(2x_1+2x_2-1)\}, \tag{14}$$

$$\gamma_1(x_1,x_2)=4\frac{\sqrt{(1-x_1)(1-x_2)(x_1+x_2-1)}(x_2-x_1)}{(2-x_1-x_2)}, \tag{15}$$

$$\gamma_2(x_1,x_2)=32\sqrt{\frac{(x_1+x_2-1)}{(1-x_1)(1-x_2)}}\frac{(x_1+x_2-1)(x_2-x_1)}{(2-x_1-x_2)}, \tag{16}$$

$$\gamma_3(x_1,x_2)=16\sqrt{\frac{(x_1+x_2-1)}{(1-x_1)(1-x_2)}}(x_1+x_2-1)(x_2-x_1), \tag{17}$$

$$\gamma_4(x_1,x_2)=8\sqrt{\frac{(x_1+x_2-1)}{(1-x_1)(1-x_2)}}(2-x_1-x_2)(x_2-x_1). \tag{18}$$

In Eq. (6) there are three classes of terms: the first contribution arises from the four-fermion coupling constants (C_{1-4}), the second from the photon-penguin coupling constants ($C_{5,6}$), and the third from interferences between the four-fermion couplings and the photon-penguin couplings (C_{7-12}). There is no interference between the photon-penguin couplings and among the four-fermion couplings by themselves in our approximation neglecting the electron mass, because the chirality of the electrons cannot be matched between these couplings. For the same reason, the scalar type coupling constants g_1 and g_2 cannot interfere with the photon-penguin coupling constants A_R and A_L. The angular dependence with respect to the polarization direction is classified into four types, namely, terms proportional to (i) 1, (ii) $\cos\theta$, (iii) $\sin\theta\cos\varphi$, and (iv) $\sin\theta\sin\varphi$. Under the parity operation (P), θ, φ transform as

$$\theta\to\pi-\theta,$$
$$\varphi\to\begin{cases}\pi-\varphi & (0\leqslant\varphi<\pi),\\ 3\pi-\varphi & (\pi\leqslant\varphi<2\pi),\end{cases} \tag{19}$$

so that terms proportional to (ii) and (iii) are P odd. On the other hand the time reversal operation (T) induces the following transformation:

$$\theta\to\theta,\quad \varphi\to2\pi-\varphi. \tag{20}$$

Thus only terms proportional to C_{11} and C_{12} are T-odd quantities. Notice that these terms are given by imaginary parts of interference terms between photon-penguin and vector type four-fermion coupling constants. This means that effects of CP violation can be seen only through a phase difference between these two coupling constants.

It is convenient to define integrated asymmetries in order to separate four angular dependences, although in principle we can determine C_i separately by fitting experimental data in full phase space. In the Dalitz plot, α_3 and β_2 have a singularity as $1/(1-x_{1,2})$ in the region near the kinematical boundary ($x_{1,2}\sim1$). γ_2, γ_3, and γ_4 have a weaker singularity as $1/\sqrt{1-x_{1,2}}$. α_3, β_2, and γ_2 arise as square of photon-penguin amplitudes whereas γ_3 and γ_4 from interferences between photon-penguin and four-fermion terms. On the contrary, contributions from square of the four-fermion coupling constants have no singularity on the edge and have a rather flat shape. These singular behaviors are cut off if we take into account the electron mass. To show this behavior explicitly, we first integrate over smaller positron energy x_2 fixing the larger positron energy x_1 and define the following differential branching ratio and three types of asymmetries a_{P_1}, a_{P_2}, and a_T as a function of the larger positron energy $x_1(\frac{1}{2}\leqslant x_1\leqslant1)$:

$$\frac{dB(x_1)}{dx_1}\equiv\int_{1-x_1}^{x_1}dx_2\int_{-1}^{1}d\cos\theta\int_0^{2\pi}d\varphi\frac{dB}{dx_1dx_2d\cos\theta d\varphi}$$
$$=3\{(C_1+C_2)F_1(x_1)+(C_3+C_4)F_2(x_1)+(C_5+C_6)F_3(x_1)+(C_7+C_8)F_4(x_1)$$
$$+(C_9+C_{10})F_5(x_1)\}, \tag{21}$$

$$a_{P_1}(x_1)\equiv \frac{1}{P\dfrac{dB(x_1)}{dx_1}}\left(\int_{1-x_1}^{x_1}dx_2\int_0^1 d\cos\theta\int_0^{2\pi}d\varphi\frac{dB}{dx_1dx_2d\cos\theta d\varphi}-\int_{1-x_1}^{x_1}dx_2\int_{-1}^{0}d\cos\theta\int_0^{2\pi}d\varphi\frac{dB}{dx_1dx_2d\cos\theta d\varphi}\right)$$

$$=\frac{3}{2}\frac{1}{\dfrac{dB(x_1)}{dx_1}}\{(C_1-C_2)F_1(x_1)+(C_3-C_4)G_1(x_1)+(C_5-C_6)G_2(x_1)-(C_7-C_8)F_4(x_1)$$

$$+(C_9-C_{10})F_5(x_1)\}, \tag{22}$$

$$a_{P_2}(x_1)\equiv \frac{-1}{P\dfrac{dB(x_1)}{dx_1}}\left(\int_{1-x_1}^{x_1}dx_2\int_{-1}^{1}d\cos\theta\int_0^{\pi/2}d\varphi\frac{dB}{dx_1dx_2d\cos\theta d\varphi}\right.$$

$$\left.-\int_{1-x_1}^{x_1}dx_2\int_{-1}^{1}d\cos\theta\int_{\pi/2}^{3/2\pi}d\varphi\frac{dB}{dx_1dx_2d\cos\theta d\varphi}+\int_{1-x_1}^{x_1}dx_2\int_{-1}^{1}d\cos\theta\int_{3/2\pi}^{2\pi}d\varphi\frac{dB}{dx_1dx_2d\cos\theta d\varphi}\right)$$

$$=\frac{3}{2}\frac{1}{\dfrac{dB(x_1)}{dx_1}}\{(C_3-C_4)H_1(x_1)+(C_5-C_6)H_2(x_1)+(C_7-C_8)H_3(x_1)$$

$$-(C_9-C_{10})H_4(x_1)\}, \tag{23}$$

$$a_T(x_1)\equiv \frac{-1}{P\dfrac{dB(x_1)}{dx_1}}\left(\int_{1-x_1}^{x_1}dx_2\int_{-1}^{1}d\cos\theta\int_0^{\pi}d\varphi\frac{dB}{dx_1dx_2d\cos\theta d\varphi}-\int_{1-x_1}^{x_1}dx_2\int_{-1}^{1}d\cos\theta\int_{\pi}^{2\pi}d\varphi\frac{dB}{dx_1dx_2d\cos\theta d\varphi}\right)$$

$$=\frac{3}{2}\frac{1}{\dfrac{dB(x_1)}{dx_1}}\{C_{11}H_3(x_1)-C_{12}H_4(x_1)\}. \tag{24}$$

In these formulas, F_i, G_i, and H_i are functions of the variable x_1 and their analytic forms are found in Appendix A. $dB(x_1)/dx_1$, $a_{P_1}(x_1)$, $a_{P_2}(x_1)$, and $a_T(x_1)$ are defined to extract terms (i)–(iv) with different angular dependences and $a_T(x_1)$ is the T-odd quantity. In the above expression $F_3(x_1)$ in $dB(x_1)/dx_1$ and $G_2(x_1)$ in a_{P_1} have $1/(1-x_1)$ singularity. Introducing the cutoff δ for variable x_1 and integrating over $\frac{1}{2}\leqslant x_1\leqslant 1-\delta$, we define the integrated branching ratio B and three asymmetries A_{P_1}, A_{P_2}, and A_T:

$$B[\delta]=\int_{1/2}^{1-\delta}dx_1\frac{dB(x_1)}{dx_1}$$

$$=3\{(C_1+C_2)I_1[\delta]+(C_3+C_4)I_2[\delta]+(C_5+C_6)I_3[\delta]+(C_7+C_8)I_4[\delta]+(C_9+C_{10})I_5[\delta]\}, \tag{25}$$

$$A_{P_1}[\delta]=\frac{1}{B[\delta]}\int_{1/2}^{1-\delta}dx_1a_1(x_1)\frac{dB}{dx_1}(x_1)$$

$$=\frac{3}{2B[\delta]}\{(C_1-C_2)I_1[\delta]+(C_3-C_4)J_1[\delta]+(C_5-C_6)J_2[\delta]-(C_7-C_8)I_4[\delta]+(C_9-C_{10})I_5[\delta]\}, \tag{26}$$

$$A_{P_2}[\delta]=\frac{1}{B[\delta]}\int_{1/2}^{1-\delta}dx_1a_2(x_1)\frac{dB}{dx_1}(x_1)$$

$$=\frac{3}{2B[\delta]}\{(C_3-C_4)K_1[\delta]+(C_5-C_6)K_2[\delta]+(C_7-C_8)K_3[\delta]-(C_9-C_{10})K_4[\delta]\}, \tag{27}$$

$$A_T[\delta]=\frac{1}{B[\delta]}\int_{1/2}^{1-\delta}dx_1a_3(x_1)\frac{dB}{dx_1}(x_1)=\frac{3}{2B[\delta]}\{C_{11}K_3[\delta]-C_{12}K_4[\delta]\}. \tag{28}$$

I_i, J_i, and K_i are functions of the cutoff δ and their analytic forms are also found in Appendix A. Note that $I_3[\delta]$ and $J_2[\delta]$ have a logarithmic singularity at $\delta=0$. Because of this logarithmic dependence, the terms $|A_L|^2$ and $|A_R|^2$ dominate over other terms in the branching ratio if coupling constants eA_L, eA_R, and g_i have similar magnitudes. On the other hand the numerator of A_T does not have a singular behavior so that A_T itself is suppressed when we take very small δ. In the latter analysis of SUSY GUT cases we introduce the cutoff δ to optimize the T-odd asymmetry.

We have to take into account the electron mass properly to get precise value of total branching ratio. If the photon-penguin contribution dominates the branching ratio, we can derive a model-independent relation between the two branching ratios [14]:

$$\frac{B(\mu^+\to e^+e^+e^-)}{B(\mu^+\to e^+\gamma)}\simeq\frac{\alpha}{3\pi}\left[\ln\left(\frac{m_\mu^2}{m_e^2}\right)-\frac{11}{4}\right]\simeq 0.0061, \tag{29}$$

where α is the fine structure constant. Neglecting the terms suppressed by m_e/m_μ, the total branching ratio is, therefore, given by

$$\begin{aligned}B(\mu^+\to e^+e^+e^-)&=2(C_1+C_2)+(C_3+C_4)\\&\quad+32\left\{\log\left(\frac{m_\mu^2}{m_e^2}\right)-\frac{11}{4}\right\}(C_5+C_6)+16(C_7+C_8)\\&\quad+8(C_9+C_{10}).\end{aligned} \tag{30}$$

III. SUSY GUT AND LFV

In this section we introduce SU(5) and SO(10) SUSY GUT and discuss LFV processes. We assume that SUSY is broken explicitly at the Planck scale with soft SUSY breaking terms and that these terms have universal structure with respect to the flavor indices as suggested by the minimal SUGRA model. First, we discuss the LFV process in the SU(5) SUSY GUT and introduce the SO(10) SUSY GUT in the next subsection.

A. SU(5) SUSY GUT

In the SU(5) SUSY GUT, we have three generations of $\mathbf{10}(T)$ and $\overline{\mathbf{5}}(\overline{F})$ representations of SU(5) as matter fields and $\mathbf{5}(H)$ and $\overline{\mathbf{5}}(\overline{H})$ representations of Higgs fields. The Yukawa superpotential and the soft SUSY breaking Lagrangian are written as follows:

$$\mathcal{W}_{\mathrm{SU(5)}}=\frac{1}{8}(y_u)_{ij}T_iT_jH+(y_d)_{ij}\overline{F}_iT_j\overline{H}, \tag{31}$$

$$\begin{aligned}\mathcal{L}_{\mathrm{soft}}&=-(m_T^2)_{ij}\tilde{T}_i^\dagger\tilde{T}_j-(m_{\overline{F}}^2)_{ij}\tilde{\overline{F}}_i^\dagger\tilde{\overline{F}}_j-m_H^2H^\dagger H\\&\quad-m_{\overline{H}}^2\overline{H}^\dagger\overline{H}-\left\{\frac{m_0}{8}(A_u)_{ij}\tilde{T}_i\tilde{T}_jH\right.\\&\quad\left.+m_0(A_d)_{ij}\tilde{\overline{F}}_i\tilde{T}_j\overline{H}+\frac{1}{2}M_5\overline{\lambda}_{5R}\lambda_{5L}+\mathrm{H.c.}\right\},\end{aligned} \tag{32}$$

where i,j are generation indices. $\tilde{T}$, $\tilde{\overline{F}}$ are scalar components of the superfields T, $\overline{F}$.

At the Planck scale these soft SUSY breaking parameters satisfy flavor-blind universal conditions which are implied in the minimal SUGRA model:

$$\begin{aligned}&m_T^2=m_{\overline{F}}^2=m_0^2\mathbf{1},\quad m_H^2=m_{\overline{H}}^2=m_0^2,\\&(A_u)_{ij}=A_0(y_u)_{ij},\quad (A_d)_{ij}=A_0(y_d)_{ij}.\end{aligned} \tag{33}$$

With these conditions the lepton and slepton mass matrices can be diagonalized simultaneously at the Planck scale, and therefore there is no LFV at this scale. However, these conditions receive corrections from the renormalization effect between the Planck scale and the GUT scale mainly due to the large top Yukawa coupling constant. As a result the magnitude of the 3-3 element of the mass matrix for **10** scalar fields becomes smaller than 1-1 and 2-2 elements. In the basis where y_u is diagonalized at the Planck scale, the mass matrix for the **10** scalar fields at the GUT scale is approximately given by

$$\begin{aligned}m_T^2&\simeq\begin{pmatrix}m^2&&\\&m^2&\\&&m^2+\Delta m^2\end{pmatrix},\\\Delta m^2&\simeq-\frac{3}{8\pi^2}|(y_u)_{33}|^2m_0^2(3+|A_0|^2)\ln\left(\frac{M_P}{M_G}\right),\end{aligned} \tag{34}$$

where M_P and M_G denote the reduced Planck mass ($\sim 2\times10^{18}$ GeV) and the GUT scale ($\sim 2\times10^{16}$ GeV). This correction amounts to about 50% of their original values and the lepton and slepton mass matrices are no longer diagonalized simultaneously. This becomes a source of LFV which could induce observable effects in $\mu^+\to e^+\gamma$ [1].

The SU(5) symmetry is broken to the SM groups at the GUT scale, and after integrating out heavy fields the effective theory becomes the minimal supersymmetric standard model (MSSM). The superpotential and the soft SUSY breaking Lagrangian for the MSSM are written as follows:

$$\begin{aligned}\mathcal{W}_{\mathrm{MSSM}}&=\epsilon^{\alpha\beta}(y_e)_{ij}H_{1\alpha}E_i^cL_{j\beta}+\epsilon^{\alpha\beta}(y_d)_{ij}H_{1\alpha}D_i^cQ_{j\beta}\\&\quad+\epsilon^{\alpha\beta}(y_u)_{ij}H_{2\alpha}U_i^cQ_{j\beta}+\epsilon^{\alpha\beta}\mu H_{1\alpha}H_{2\beta},\end{aligned} \tag{35}$$

$$\begin{aligned}\mathcal{L}_{\rm soft} = & -(m_E^2)_{ij}\tilde{E}_i^*\tilde{E}_j - (m_L^2)_{ij}\tilde{L}_i^*\tilde{L}_j - (m_D^2)_{ij}\tilde{D}_i^*\tilde{D}_j \\ & -(m_U^2)_{ij}\tilde{U}_i^*\tilde{U}_j - (m_Q^2)_{ij}\tilde{Q}_i^*\tilde{Q}_i - m_{H_1}^2 H_1^\dagger H_1 \\ & -m_{H_2}^2 H_2^\dagger H_2 - \Big[m_0(A_e)_{ij}\epsilon^{\alpha\beta}H_{1\alpha}\tilde{E}_i^*\tilde{L}_{j\beta} \\ & + m_0(A_d)_{ij}\epsilon^{\alpha\beta}H_{1\alpha}\tilde{D}_i^*\tilde{Q}_{j\beta} \\ & + m_0(A_u)_{ij}\epsilon^{\alpha\beta}H_{2\alpha}\tilde{U}_i^*\tilde{Q}_{j\beta} + \epsilon^{\alpha\beta}\mu B H_{1\alpha}H_{2\beta} \\ & + \frac{1}{2}M_1\bar{\tilde{B}}_R\tilde{B}_L + \frac{1}{2}M_2\bar{\tilde{W}}_R\tilde{W}_L + \frac{1}{2}M_3\bar{\tilde{G}}_R\tilde{G}_L \\ & + \text{H.c.}\Big]. \end{aligned} \tag{36}$$

In this formula $\epsilon^{\alpha\beta}$ is defined as $\epsilon^{11}=\epsilon^{22}=0$, $\epsilon^{12}=-\epsilon^{21}=1$. At the GUT scale these parameters satisfy the GUT relations

$$y_e = y_d^T, \tag{37}$$

$$A_e = A_d^T, \tag{38}$$

$$m_E^{2T} = m_U^{2T} = m_Q^2 = m_T^2, \quad m_L^2 = m_D^2 = m_F^2,$$

$$m_{H_1}^2 = m_H^2, \quad m_{H_2}^2 = m_H^2, \quad M_1 = M_2 = M_3 = M_5. \tag{39}$$

In the basis where y_u is diagonalized at the Planck scale, y_u at the GUT scale still approximately remains diagonal. In this basis, y_e is diagonalized in the following way:

$$V_R y_e V_L^\dagger = \text{diagonal}, \tag{40}$$

where V_L and V_R are unitary matrices and using Eq. (37) V_R is given by

$$(V_R)_{ij} = (V_{\rm KM}^0)_{ji}, \tag{41}$$

where $V_{\rm KM}^0$ is the Kobayashi-Maskawa (KM) matrix at the GUT scale.

It is useful to make unitary transformations on E_i and L_j to go to the basis where y_e is diagonalized at the GUT scale. In the new basis the off-diagonal element of m_E^2 is given by

$$(m_E^2)_{ij} \simeq -\frac{3}{8\pi^2}(V_{\rm KM}^0)_{3i}(V_{\rm KM}^0)_{3j}^* |(y_u)_{33}|^2 m_0^2 \times (3+|A_0|^2)\ln\left(\frac{M_P}{M_G}\right). \tag{42}$$

The off-diagonal element of the slepton mass matrix becomes a source of LFV.

In the actual numerical analysis, we solved the MSSM renormalization group equation from the GUT scale to the electroweak scale and determine the masses and mixings for SUSY particles. We also require that the electroweak symmetry breaking occur properly to give the correct Z-boson mass. From the MSSM Lagrangian at the electroweak scale we can derive the LFV coupling constants $A_{L,R}$ and g_{1-6} through one-loop diagrams involving slepton, gaugino, and Higgsino. The complete formulas are given in Appendix B 2.

In the SU(5) model, only the right-handed slepton mass matrix can develop off-diagonal terms if the ratio of vacuum expectation values of two Higgs fields ($\tan\beta = \langle H_2^0\rangle / \langle H_1^0\rangle$) is not very large. In such a case only A_L, g_3, and g_5 have sizable contributions. Restricting to small or moderate $\tan\beta$ cases, all effective coupling constants are proportional to the product of the KM matrix element $\lambda_\tau = (V_{\rm KM}^0)_{32}(V_{\rm KM}^0)_{31}^*$ since the LFV transition occurs through $(m_E^2)_{21}$ or $(m_E^2)_{32}^*(m_E^2)_{31}$. This situation does not change even if we take into account the LFV transition due to the left-right mixing of the slepton mass matrix. This means that the CP violating phase of Yukawa coupling constants cannot make a phase difference between A_L and g_3, or A_L and g_5, and therefore the T-odd asymmetry A_T cannot appear from this source.

There is another important source of CP violating phases in soft SUSY breaking terms. Within the SUGRA model, we can introduce four phases: phases of M_5, A_0, B, and μ, but not all of them are physically independent. By field redefinition, we can take the phases of A_0 and μ as independent phases. If we take into account these phases, A_T can be generated. Since these phases also induce the electron, neutron, and Hg EDMs [15,16], we take into account these EDM constraints to obtain allowed regions of SUSY phases.

Up to now we consider that the Yukawa coupling constants are given by Eq. (31), so that the lepton and down-type quark Yukawa coupling constants are related at the GUT scale by Eq. (37). On the other hand, it is known that this relation does not reproduce realistic mass relations for charged leptons and down-type quarks in the first and second generations. It is therefore important to study how the prediction for LFV processes depends on details of the origin of the Yukawa coupling constant in the MSSM Lagrangian. One way to generate realistic mass matrix is to introduce higher-dimensional operators in the SU(5) superpotential. Once this is done the simple relationship between the charged lepton and down-type quark Yukawa coupling constants does not hold. Although the effect of higher dimensional operators is suppressed by $O(M_G/M_P)$, masses and mixings for the first and second generations can receive large corrections to the GUT relation. If $\tan\beta$ is not very large, LFV is still induced only for the right-handed slepton sector and Eq. (42) holds with replacement of $V_{\rm KM}^0$ by V_R^T which is not necessarily related to the KM matrix elements. In the following, therefore, we treat λ_τ as a free parameter. Since the $\mu^+ \to e^+\gamma$ and the $\mu^+ \to e^+e^+e^-$ branching ratios are proportional to $|\lambda_\tau|^2$, we present these branching ratios divided by $|\lambda_\tau|^2$. If $\tan\beta$ is as large as 30, the bottom Yukawa coupling constant can induce the LFV in the left-handed slepton sector. In such a case, if we include the effect of higher-dimensional operators at the GUT scale, there are photon-penguin diagrams which are proportional to m_τ and these contributions tend to dominate over other contributions as shown in Ref. [17]. Because the LFV branching ratios depend on many unknown parameters in such a case, we do not consider this possibility here.

B. SO(10) SUSY GUT

In the minimal SO(10) model, we assume three generations of **16** representation matter fields (Ψ_i) and two **10** representation Higgs fields (Φ_u, Φ_d) of SO(10). The Yukawa superpotential and the soft SUSY breaking Lagrangian are written as follows:

$$\mathcal{W}_{\mathrm{SO(10)}} = \frac{1}{2}(y_u)_{ij}\Psi_i\Phi_u\Psi_j + \frac{1}{2}(y_d)_{ij}\Psi_i\Phi_d\Psi_j, \quad (43)$$

$$\begin{aligned}\mathcal{L}_{\mathrm{soft}} = &-(m^2_\Psi)_{ij}\tilde{\Psi}^\dagger_i\tilde{\Psi}_j - m^2_{\Phi_u}\Phi^\dagger_u\Phi_u - m^2_{\Phi_d}\Phi^\dagger_d\Phi_d \\ &-\left\{\frac{m_0}{2}(A_u)_{ij}\tilde{\Psi}_i\Phi_u\tilde{\Psi}_j + \frac{m_0}{2}(A_d)_{ij}\tilde{\Psi}_i\Phi_d\tilde{\Psi}_j \right. \\ &\left. + \frac{1}{2}M_{10}\overline{\lambda_{10R}}\lambda_{10L} + \mathrm{H.c.}\right\}. \quad (44)\end{aligned}$$

At the Planck scale, we have the universal boundary conditions

$$m^2_\Psi = m^2_0\mathbf{1}, \quad m^2_{\Phi_u} = m^2_{\Phi_d} = m^2_0, \quad (A_u)_{ij} = A_0(y_u)_{ij},$$

$$(A_d)_{ij} = A_0(y_d)_{ij}. \quad (45)$$

In contrast with the SU(5) SUSY GUT, all matter fields are unified in a single representation Ψ of SO(10) and masses of all squarks and sleptons of the third generation receive a large correction due to the renormalization effect by the top Yukawa coupling constant. In the y_u-diagonalized basis, difference between the mass of the third generation sfermion and that of the first and second generation is given by:

$$\Delta m^2_\Psi \simeq -\frac{5}{8\pi^2}|(y_u)_{33}|^2 m^2_0(3+|A_0|^2)\ln\left(\frac{M_P}{M_G}\right). \quad (46)$$

At the GUT scale, the initial conditions for the parameters of MSSM Lagrangian in Eqs. (35) and (36) at the GUT scale are written as follows:

$$y_e = y_d, \quad (47)$$

$$A_e = A_d, \quad (48)$$

$$m^2_E = m^2_L = m^2_D = m^2_U = m^2_Q = m^2_\Psi,$$

$$m^2_{H_1} = m^2_{\Phi_d}, \quad m^2_{H_2} = m^2_{\Phi_u}, \quad M_1 = M_2 = M_3 = M_{10}, \quad (49)$$

where the symmetric matrix y_e can be expressed as

$$y_e = U^T P \hat{y}_e U,$$

$$P = \begin{pmatrix} e^{i\phi_1} & & \\ & e^{i\phi_2} & \\ & & e^{i\phi_3} \end{pmatrix}, \quad (50)$$

where $\hat{y}_e$ is a real diagonal matrix, and therefore the unitary matrix U is related to the KM matrix at the GUT scale as

$$U = V^{0\dagger}_{\mathrm{KM}}. \quad (51)$$

If we go to the y_e-diagonalized basis at the GUT scale, the off-diagonal elements of slepton mass matrices become as follows:

$$\begin{aligned}(m^2_E)_{ij} \simeq &-\frac{5}{8\pi^2}e^{-i(\phi_i-\phi_j)}(V^0_{\mathrm{KM}})_{3i}(V^0_{\mathrm{KM}})^*_{3j}|(y_u)_{33}|^2 m^2_0 \\ &\times(3+|A_0|^2)\ln\left(\frac{M_P}{M_G}\right), \quad (52)\end{aligned}$$

$$\begin{aligned}(m^2_L)_{ij} \simeq &-\frac{5}{8\pi^2}(V^0_{\mathrm{KM}})^*_{3i}(V^0_{\mathrm{KM}})_{3j}|(y_u)_{33}|^2 m^2_0 \\ &\times(3+|A_0|^2)\ln\left(\frac{M_P}{M_G}\right). \quad (53)\end{aligned}$$

Since the left-handed slepton also has the LFV effect in the case of the SO(10) SUSY GUT, there are dominant photon-penguin diagrams which are proportional to m_τ in the slepton left-right mixing as discussed in Ref. [2] .

In addition to the KM phase, there are two physical phases in Eq. (50) up to an overall phase. A combination of these phases and the KM phase is responsible to the electron EDM [2,18]. If the photon-penguin diagram proportional to m_τ dominates in the $\mu^+ \to e^+\gamma$ amplitude, there is a simple relation between the electron EDM and the $\mu^+ \to e^+\gamma$ branching ratio [2]. Defining a phase as

$$\begin{aligned}&\mathrm{Im}[e^{i(\phi_3-\phi_1)}\{(V^0_{\mathrm{KM}})_{31}(V^0_{\mathrm{KM}})^*_{33}\}^2] \\ &\quad = |(V^0_{\mathrm{KM}})_{31}(V^0_{\mathrm{KM}})^*_{33}|^2 \sin\phi, \quad (54)\end{aligned}$$

the relation is given by

$$|d_e| = 1.3\sqrt{\frac{B(\mu\to e\gamma)}{10^{-12}}}|\sin\phi| \quad (10^{-27} e\ \mathrm{cm}). \quad (55)$$

Later we see that the diagram proportional to m_τ does not necessarily dominate over other diagrams. In such a case the above relation does not hold.

IV. RESULTS OF NUMERICAL CALCULATIONS

We present results of our numerical analysis on $\mu^+ \to e^+\gamma$ and $\mu^+ \to e^+e^+e^-$ processes for the SU(5) and SO(10) SUSY GUT. We also calculate the electron, neutron, and Hg EDMs as constraints on the CP violating phases of the soft SUSY breaking terms. Following the procedure discussed in the previous section, we solve the renormalization

group equations with the universal condition for the SUSY breaking terms at the Plank scale. Though the approximate formulas for the slepton mass difference are given in the previous section to explain qualitative features, we solve the renormalization group equations from the Planck scale to the electroweak scale numerically taking into account the full flavor-mixing matrix for fermions and sfermions. To determine allowed range of SUSY parameter space we use the results of various SUSY particle searches at LEP and Tevatron and the branching ratio $B(b \to s\gamma)$. The details on these constraints are described in Ref. [19].[1] We take the top quark mass as $m_t = 175$ GeV. Because we calculate the LFV branching ratios divided by $|\lambda_\tau|^2$, the result is almost independent of the KM matrix elements. For definiteness, we use the input parameters of the KM matrix elements as $|(V_{\rm KM})_{cb}| = 0.041$, $|(V_{\rm KM})_{td}| = 0.006$, and $|(V_{\rm KM})_{us}| = 0.22$. Requiring the radiative electroweak symmetry breaking the free parameters of the supergravity (SUGRA) model can be taken as $\tan\beta$, M_2, m_0, $|A_0|$ and the phase of A_0 (θ_{A_0}) and that of μ (θ_μ).

A. SU(5) GUT

Let us first discuss the case without the CP violating phases in the SU(5) GUT. In Fig. 3 we present the following quantities:

$$\frac{B(\mu^+ \to e^+\gamma)}{|\lambda_\tau|^2},\ \frac{B(\mu^+ \to e^+e^+e^-)}{|\lambda_\tau|^2},\ \frac{B(\mu^+ \to e^+e^+e^-)}{B(\mu^+ \to e^+\gamma)},$$

$$A(\mu^+ \to e^+\gamma),\ A_{P_1},\ A_{P_2}, \tag{56}$$

in the plane of $m_{\tilde{e}_R}$ and $|A_0|$ for $\tan\beta = 3$, $M_2 = 150$ GeV, $\theta_{A_0} = \theta_\mu = 0$. Here λ_τ is defined by the mixing matrix which diagonalizes the right-handed slepton mass matrix at the electroweak scale in the basis where the charged lepton mass matrix is diagonalized. For the asymmetries we take the cutoff parameter $\delta = 0.02$. If $|\lambda_\tau| = 10^{-2}$, $B(\mu^+ \to e^+\gamma)$ can be 10^{-11} and $B(\mu \to e^+e^+e^-)$ can be 10^{-13} level, but if λ_τ is given by the corresponding KM matrix element, $|\lambda_\tau|$ becomes $(3\text{–}5)\times 10^{-4}$, so that the branching ratios are smaller by three orders of magnitude. In Fig. 3(c) the ratio of two branching fractions is shown. If the photon-penguin contribution dominates over four-fermion ones this ratio is given by Eq. (29). We can see that for large parameter region the ratio is enhanced. In particular, near $m_{\tilde{e}_R} = 400$–600 GeV almost exact cancellation occurs for the photon-penguin amplitudes [3]. In Fig. 3(d) $A(\mu^+ \to e^+\gamma)$ is shown. It is close to 100% except for small region where the almost exact cancellation occurs. The P-odd asymmetries A_{P_1} and A_{P_2} are shown in Figs. 3(e) and 3(f). A_{P_1} changes from -30 to 40 % and A_{P_2} changes from -10 to 15 %. For $\delta = 0.02$ the asymmetries A_{P_1} and A_{P_2} are expressed as

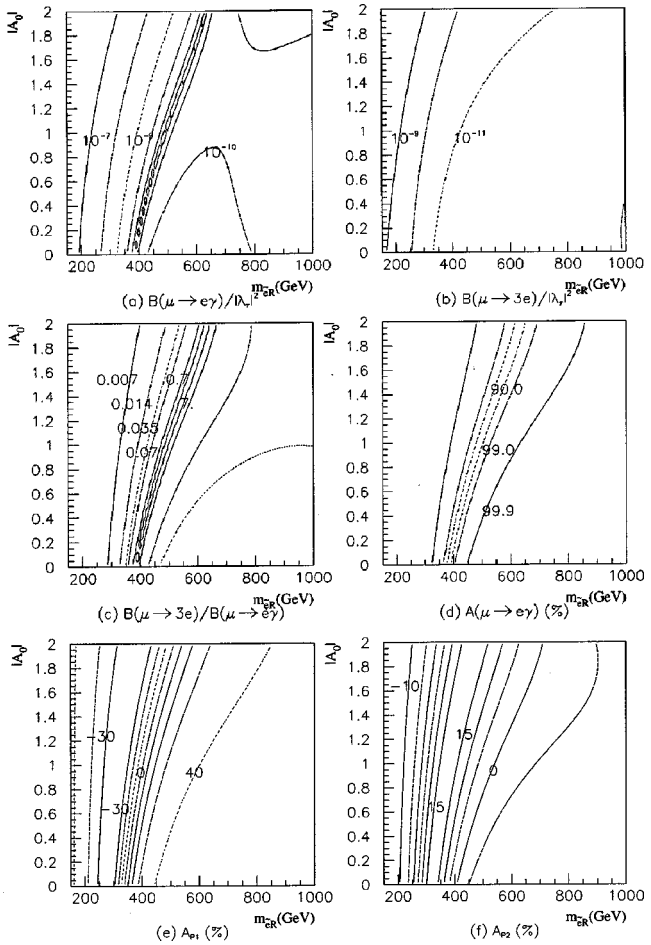

FIG. 3. The observables in the SU(5) model without the SUSY CP violating phases in the $m_{\tilde{e}_R}$-$|A_0|$ plane. We fix the SUSY parameters as $\tan\beta = 3$, $M_2 = 150$ GeV, and $\mu > 0$ and the top quark mass as 175 GeV. (a) Branching ratio for $\mu^+ \to e^+\gamma$ normalized by $|\lambda_\tau|^2 \equiv |(V_R)_{23}(V_R)^*_{13}|^2$. (b) Branching ratio for $\mu^+ \to e^+e^+e^-$ normalized by $|\lambda_\tau|^2$. (c) The ratio of two branching fractions $B(\mu \to 3e)/B(\mu \to e\gamma)$. (d) The P-odd asymmetry for $\mu^+ \to e^+\gamma$. (e) The P-odd asymmetries A_{P_1} for $\mu^+ \to e^+e^+e^-$. (f) The P-odd asymmetries A_{P_2} for $\mu^+ \to e^+e^+e^-$. The cutoff parameter δ is taken to be 0.02.

$$A_{P_1} \simeq \frac{3}{2B}\{0.6(C_1 - C_2) - 0.12(C_3 - C_4) + 5.6(C_5 - C_6) - 4.7(C_7 - C_8) + 2.5(C_9 - C_{10})\}, \tag{57}$$

$$A_{P_2} \simeq \frac{3}{2B}\{0.1(C_3 - C_4) + 10(C_5 - C_6) + 2(C_7 - C_8) - 1.6(C_9 - C_{10})\}. \tag{58}$$

In the SU(5) case, because only g_3, g_5, and A_L have sizable contributions, we obtain the following expressions:

[1]The branching ratio $B(b \to s\gamma)$ is updated as $2.0\times 10^{-4} < B(B \to X_s\gamma) < 4.5\times 10^{-4}$ [20].

$$A_{P_1} \simeq \frac{3}{2B}\{0.6|g_3|^2 - 0.12|g_5|^2 - 5.6|eA_L|^2 + 4.7\,\mathrm{Re}(eA_L g_3^*) - 2.5\,\mathrm{Re}(eA_L g_5^*)\}, \quad (59)$$

$$A_{P_2} \simeq \frac{3}{2B}\{0.1|g_5|^2 - 10|eA_L|^2 - 2\,\mathrm{Re}(eA_L g_3^*) + 1.6\,\mathrm{Re}(eA_L g_5^*)\}. \quad (60)$$

In the above formulas we can see that the coefficients for $|A_L|^2$, $\mathrm{Re}(A_L g_3^*)$, and $\mathrm{Re}(A_L g_5^*)$ are large. Therefore these asymmetries represent the dependence of square of photon-penguin terms and interference terms. It is interesting to see that we can overdetermine the three coupling constants g_3, g_5, and A_L from observables $B(\mu^+ \to e^+\gamma)$, $B(\mu^+ \to e^+e^+e^-)$, A_{P_1}, and A_{P_2} if we assume the SU(5) SUSY GUT without the SUSY CP violating phases. For example, we can determine g_3, g_5, and A_L from the three observables $B(\mu^+ \to e^+\gamma)$, $B(\mu \to e^+e^+e^-)$, and A_{P_1}, then, A_{P_2} can be predicted. In addition we should have $A(\mu^+ \to e^+\gamma) = 100\%$ and $A_T = 0$.

Next, we include the SUSY CP violating phases and discuss EDM constraints and T-odd asymmetry. We calculate the electron and neutron EDMs according to Ref. [21]. Discussion on QCD correction is given in Appendix D. For the Hg EDM, we use the result of Ref. [16]. d_{Hg} is given

$$d_{Hg} = -(C_d^C - C_u^C - 0.012 C_s^C) \times 3.2 \times 10^{-2} e, \quad (61)$$

where C_u^C, C_d^C, and C_s^C are chromomagnetic moments discussed in Appendix D.

In order to see θ_{A_0} and θ_μ dependences on the EDMs and A_T, we first show these quantities for a specific set of SUSY parameters. In Fig. 4, the electron, neutron, and Hg EDMs and A_T are shown for $\tan\beta = 3$, $M_2 = 300$ GeV, $m_{\tilde{e}_R} = 650$ GeV, $|A_0| = 1$ in the parameter region $-\pi < \theta_{A_0} \leq \pi$ and $-0.05\pi \leq \theta_\mu \leq 0.05\pi$. The experimental bounds on the EDMs are given by $|d_e| < 4 \times 10^{-27}(e\ \mathrm{cm})$ [22], $|d_n| < 0.63 \times 10^{-25}(e\ \mathrm{cm})$ [23], and $|d_{Hg}| < 9 \times 10^{-28}(e\ \mathrm{cm})$ [24]. As is well known in Ref. [25] the EDMs are very sensitive to θ_μ, so that θ_μ is strongly constrained. On the other hand θ_{A_0} can be large. In this particular parameter set, $\theta_{A_0} = \pi/2$ is not excluded by three EDM constraints. Maximum value of the T-odd asymmetry A_T in allowed region in this figure is 15%. Note that A_T is proportional to $\sin\theta_{A_0}$ in a good approximation because the magnitude of θ_μ is strongly constraint by the EDMs.

In Fig. 5 we show the quantities in Eq. (56) and A_T for $\tan\beta = 3$, $M_2 = 300$ GeV, $\theta_{A_0} = \pi/2$, $\theta_\mu = 0$. We also show the constraints from the electron, neutron, and Hg EDMs. Within the EDM constraints A_T can be 10%. As discussed in Fig. 4, when we vary θ_μ around $\theta_\mu = 0$, the EDM values change considerably but A_T is almost constant. Therefore the allowed region by the EDM constraints moves in Fig. 5 if we take θ_μ as slightly different value from 0. On the other hand the contours for branching ratios and the asymmetries in this figure are almost exactly the same. In this figure we also show the parameter region which is not allowed by the EDM constraints even if we change θ_μ around $\theta_\mu = 0$ for $\theta_{A_0} = \pi/2$. Within the allowed region, the maximum value of A_T is 15%. Similar plots are shown for $\tan\beta = 10$ in Fig. 6. In this case also the maximum value of A_T is about 15%. Note that, in the case with the CP violating phases, we can still determine the complex coupling constants g_3, g_5, and A_L up to a total phase from the two branching ratios $B(\mu^+ \to e^+\gamma)$, $B(\mu^+ \to e^+e^+e^-)$ and three asymmetries A_{P_1}, A_{P_2}, and A_T.

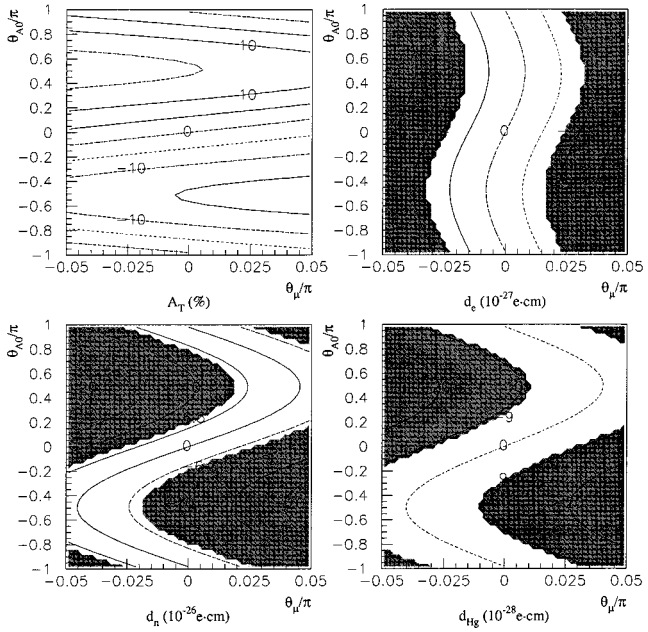

FIG. 4. θ_{A_0} and θ_μ dependences on the EDMs and A_T. We take a specific set of SUSY parameters $\tan\beta = 3$, $M_2 = 300$ GeV, $m_{\tilde{e}_R} = 650$ GeV, and $|A_0| = 1$ in the parameter region $-\pi < \theta_{A_0} \leq \pi$ and $-0.05\pi \leq \theta_\mu \leq 0.05\pi$. Dark shaded regions are excluded by the EDM experiments.

B. SO(10) GUT

In the SO(10) case, from Eq. (50), there are two physical phases which contribute to the EDMs and $\mu^+ \to e^+\gamma$ amplitudes. In the $\mu^+ \to e^+\gamma$ amplitudes the term proportional to m_τ has a dependence of $e^{i(\phi_3 - \phi_2)}(V^0_{\mathrm{KM}})_{32}\{(V^0_{\mathrm{KM}})^*_{33}\}^2(V^0_{\mathrm{KM}})_{31}$ and other contributions are proportional to $(V^0_{\mathrm{KM}})^*_{32}(V^0_{\mathrm{KM}})_{31}$. Therefore, the branching ratio $\mu^+ \to e^+\gamma$ depends on the relative phase of two terms. In the following we consider the case where there is no relative phase so that the amplitude is proportional to λ_τ. Also we do not consider EDM constraints from Eq. (55) explicitly since this can be suppressed when ϕ is small.

In Fig. 7 the branching ratios and the asymmetries are shown for the SO(10) model. We first show the case without the SUSY CP violating phases. Input SUSY parameters are taken as $\tan\beta = 3$, $M_2 = 150$ GeV, $\theta_{A_0} = 0$, and $\theta_\mu = 0$. We see that $B(\mu^+ \to e^+\gamma)/|\lambda_\tau|^2$ can be 10^{-3}. This value is enhanced by 2–4 orders of magnitude compared to the SU(5)

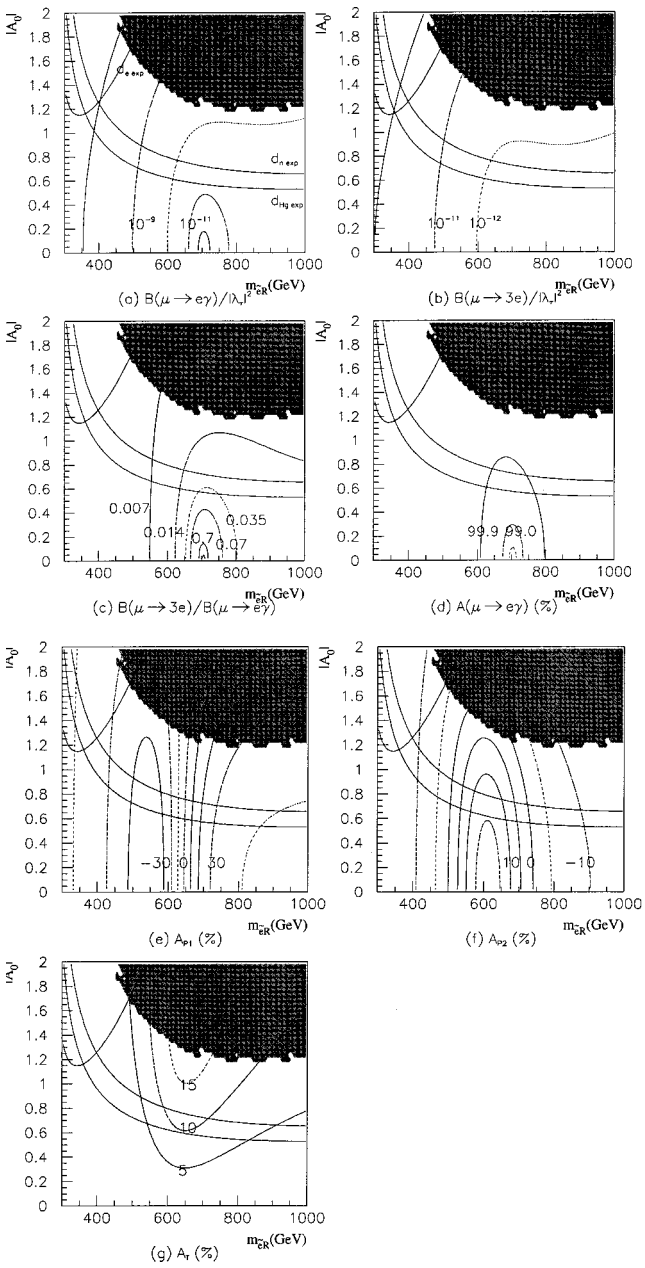

FIG. 5. The observables in the SU(5) model with the SUSY *CP* violating phases in the $m_{\tilde{e}_R}$-$|A_0|$ plane. We fix the SUSY parameters as $\tan\beta=3$, $M_2=300$ GeV, $\theta_{A_0}=\pi/2$, and $\theta_\mu=0$ and the top quark mass as 175 GeV. (a)–(f) are the same as Fig. 3. (g) The *T*-odd asymmetry for $\mu^+ \to e^+e^+e^-$. The cutoff parameter δ is taken to be 0.02. The experimental bounds from the electron, neutron, and Hg EDMs are also shown in each figure. The left upper line corresponds to the electron EDM, the right upper line to the neutron EDM, and the right lower line to the Hg EDM. The lower side of each bound is allowed by these experiments. A dark shaded region is excluded by the EDM bounds even if we allow θ_μ taking slightly different value from 0.

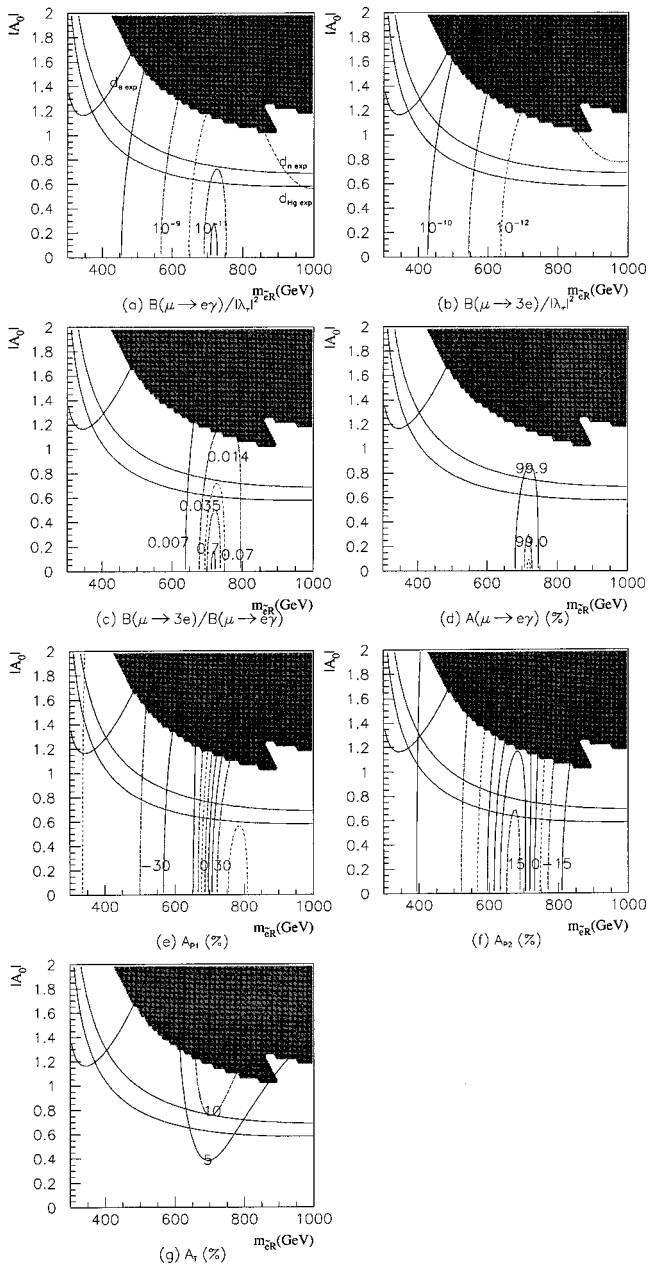

FIG. 6. The observables in the SU(5) model for $\tan\beta=10$ in $m_{\tilde{e}_R}$-$|A_0|$ plane. Other parameters are the same as in Fig. 5.

case. The ratio of two branching fractions is almost constant because the photon-penguin diagrams give dominant contributions to $\mu^+ \to e^+e^+e^-$. The $\mu^+ \to e^+\gamma$ asymmetry $A(\mu^+ \to e^+\gamma)$ varies from -20 to $-90\,\%$. This is in contrast to the previous belief that A_L and A_R have a similar magnitude in this model. Although the diagram proportional to m_τ gives the same contribution to the A_L and A_R, there is a chargino loop diagram which only contributes to A_R. In spite of no m_τ enhancement, the contribution from the latter diagram can be comparable to that from the former one, especially when the slepton mass is larger than the chargino mass. The dominant contributions to A_L and A_R are discussed based on approximate formulas in a special parameter region in Appendix C. In Figs. 7(e) and 7(f) the *P*-odd asymmetries for $\mu^+ \to e^+e^+e^-$ are shown and these asymmetries are small compared to the SU(5) case. A_{P1} is less than 10% and A_{P2} is less than 14%. In this case C_5 and C_6 terms dominate in Eqs. (57) and (58) so that these asymmetries are proportional to $A(\mu^+ \to e^+\gamma)$ and expressed as follows:

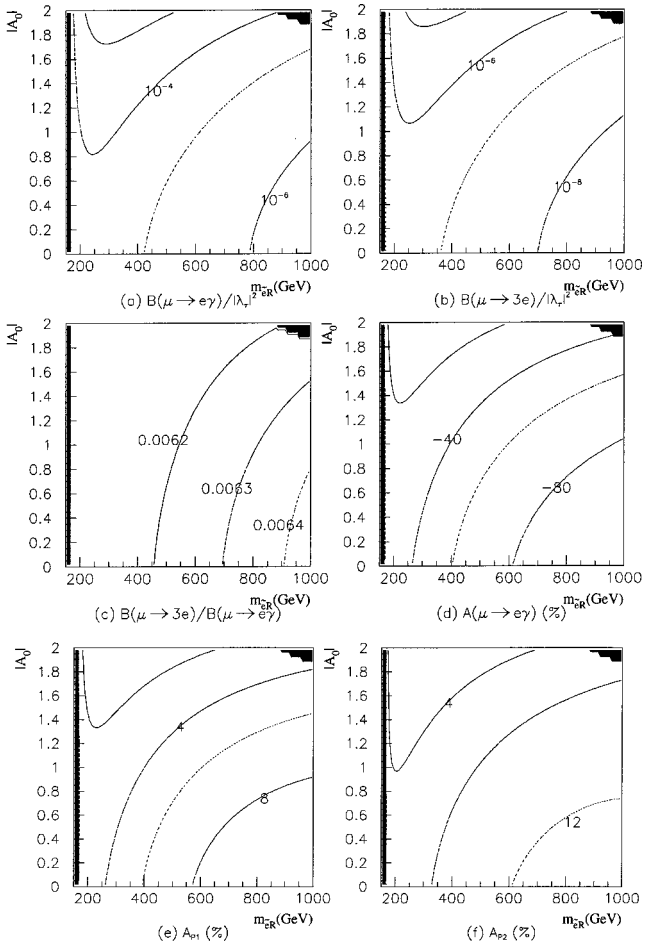

FIG. 7. The observables in the SO(10) model without the SUSY *CP* violating phase in $m_{\tilde{e}_R}$-$|A_0|$ plane. The input parameters are the same as in Fig. 3. The upper right black region is excluded by phenomenological constraints and the left black region is not allowed in the minimal SUGRA model.

$$A_{P_1} \simeq -\frac{1}{10} A(\mu^+ \to e^+ \gamma), \tag{62}$$

$$A_{P_2} \simeq -\frac{1}{6} A(\mu^+ \to e^+ \gamma). \tag{63}$$

It is interesting to see that we can predict two observables in the $\mu^+ \to e^+ e^+ e^-$ process from the $\mu^+ \to e^+ \gamma$ asymmetry. We have also investigated the case with $\tan\beta = 10$. We found the parity asymmetry for $\mu^+ \to e^+ \gamma$ and A_{P1}, A_{P2} have a similar magnitudes as Fig. 7, namely, $A(\mu^+ \to e^+ \gamma)$ varies $-20 - -100\,\%$, A_{P1} varies 2–10 % and A_{P2} varies 4–16 % in the same parameter space.

In Fig. 8 we consider the case with the SUSY *CP* violating phase and take input parameters as $\tan\beta = 3$, $M_2 = 300$ GeV, $\theta_{A_0} = \pi/2$, and $\theta_\mu = 0$. The branching ratio and other asymmetries have similar magnitudes compared to the case in Fig. 7. We can see that the *T*-odd asymmetry A_T is less than 0.01% because only the photon-penguin amplitude becomes large.

Some remarks are in order.

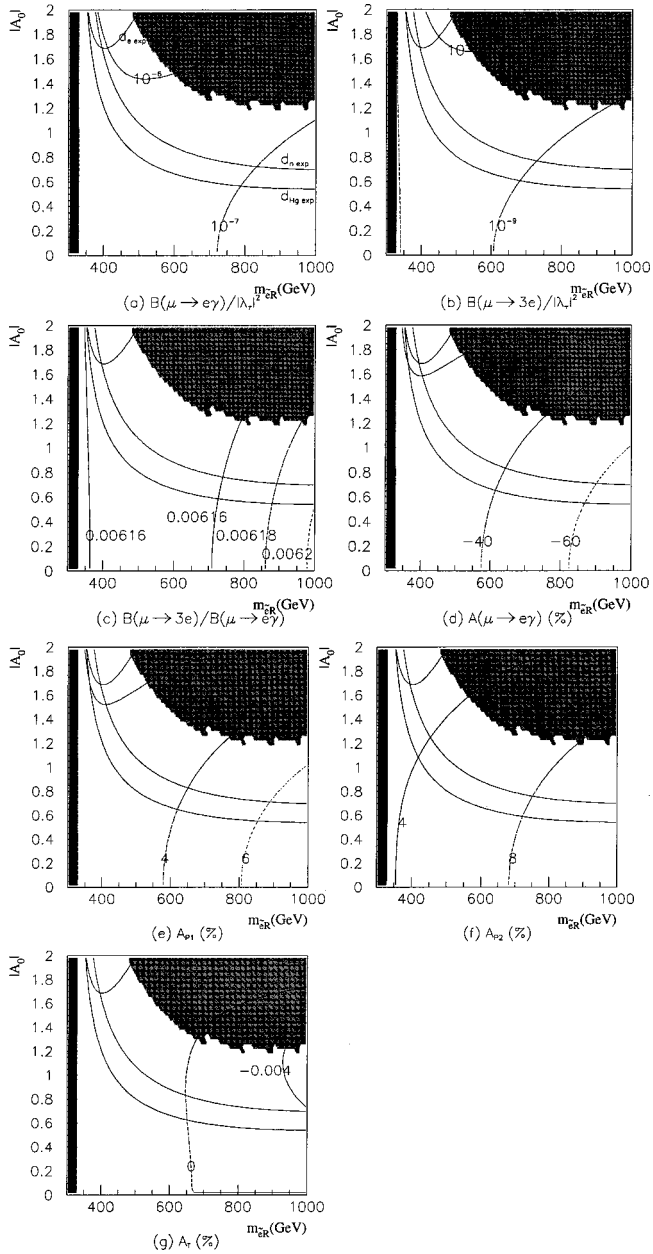

FIG. 8. The obsevables in the SO(10) model with the SUSY *CP* violating phase in $m_{\tilde{e}_R}$-$|A_0|$ plane. The input parameters are the same as in Fig. 5.

(1) When we take into account the phase in Eq. (54), the EDM is generated as discussed in Eq. (55). We note that the *T*-odd asymmetry cannot be large even in such a case because the photon-penguin diagram dominates over the four-fermion contributions.

(2) If the $\mu^+ \to e^+ \gamma$ asymmetry is sizable, the simple relationship between the EDM and the $\mu^+ \to e^+ \gamma$ branching ratio as in Eq. (55) does not hold. This is because the EDM amplitude is no longer proportional to the $\mu^+ \to e^+ \gamma$ amplitude due to the chargino loop contribution.

(3) Even if we include relative phases between the term proportional to m_τ and other contributions in the $\mu^+ \to e^+ \gamma$ amplitude, we expect large $A(\mu^+ \to e^+ \gamma)$ as long as two contributions have a similar magnitude. By numerical calcu-

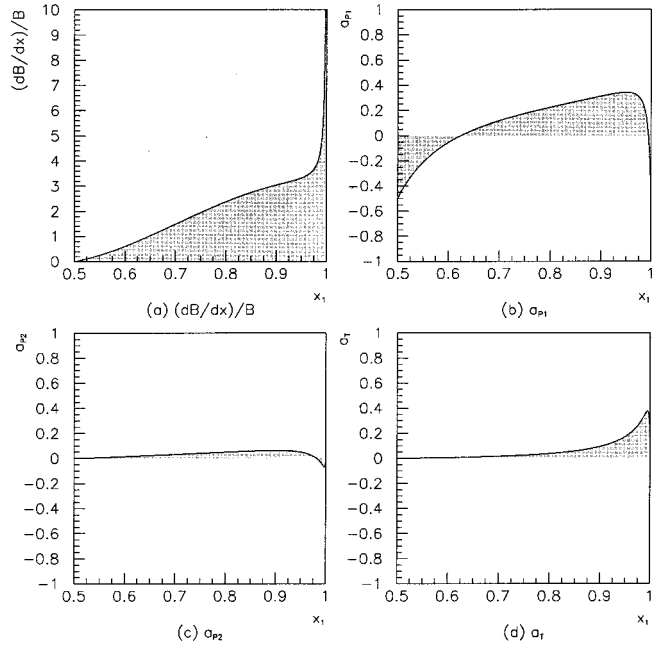

FIG. 9. The differential branching ratio and asymmetries for the $\mu^+ \to e^+e^+e^-$ process in the SU(5) model as a function of x_1 which is a larger energy of decay positrons ($2E_1/m_\mu$). We fix the SUSY parameters as $\tan\beta = 3$, $M_2 = 300$ GeV, $m_{\tilde{e}_R} = 700$ GeV, $|A_0| = 0.5$, $\theta_{A_0} = \pi/2$, and $\theta_\mu = 0$. (a) The differential branching ratio for the $\mu^+ \to e^+e^+e^-$ normalized by the total branching ratio. (b) The differential P-odd asymmetry a_{P_1}. (c) The differential P-odd asymmetry a_{P_2}. (d) The differential T-odd asymmetry a_T.

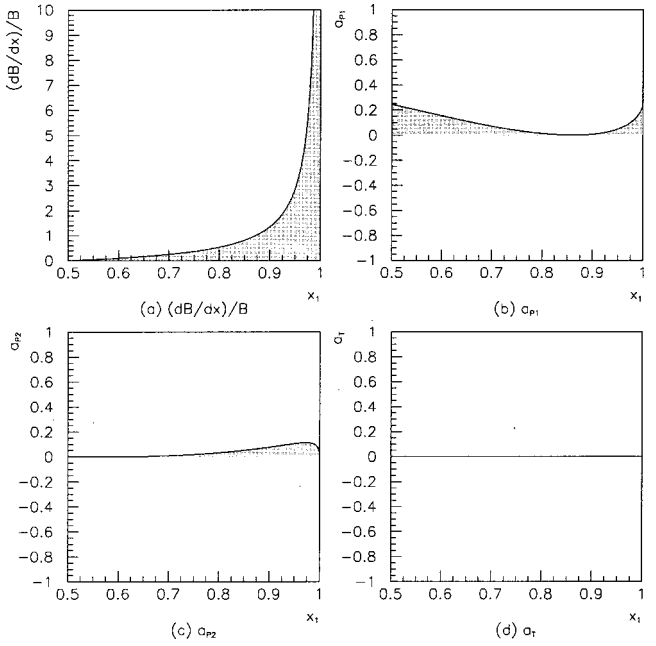

FIG. 10. The differential branching ratio and asymmetries for the $\mu^+ \to e^+e^+e^-$ process in the SO(10) model as a function of x_1. The input parameters are the same as in Fig. 9.

lation we have checked that the asymmetry varies from -100 to 100 % if we include the relative phases. Qualitatively, this feature can be understood by the approximate formulas in Appendix C. From Eq. (C1) we can see that the neutralino and chargino contributions to A_R can interfere either constructively or destructively depending on the relative phase so that $A(\mu^+ \to e^+\gamma)$ can change its sign.

C. Differential branching ratio and asymmetries

Up to now we only discussed the integrated branching ratio and asymmetries of $\mu^+ \to e^+e^+e^-$. In the actual experiment, the differential quantities are useful to distinguish different models. For example, in Figs. 9 and 10, we show the differential branching ratio and asymmetries for a particular parameter set in the SU(5) and SO(10) models. dB/dx_1, a_{P_1}, a_{P_2}, and a_T are plotted for the parameter set of $\tan\beta = 3$, $m_{\tilde{e}_R} = 700$ GeV, $M_2 = 300$ GeV, $|A_0| = 0.5$, $\theta_{A_0} = \pi/2$, and $\theta_\mu = 0$. We can see clear differences between the SU(5) and SO(10) models. The differential branching has the steep peak near $x_1 = 1$ for the SO(10) case whereas the distribution is broader for the SU(5) case. This is because the photon-penguin contribution has $1/(1-x_1)$ behavior near $x_1 = 1$ and the four-fermion operators give a broad spectrum. We also see the T-odd asymmetry has the peak at x_1 close to 1. This fact arises from the $1/\sqrt{1-x_1}$ behavior in the γ_3 and γ_4 near $x_1 = 1$. Because of this feature of distribution, we have chosen $\delta = 0.02$ to optimize the T-odd asymmetry.

V. CONCLUSION

We developed the model-independent formalism for the process $\mu^+ \to e^+\gamma$ and $\mu^+ \to e^+e^+e^-$ with polarized muon and defined convenient observables such as the P-odd and T-odd asymmetries. Using explicit calculation based on the SU(5) and SO(10) SUSY GUT, we show that various combination of LFV coupling constants can be determined from the measurement of branching ratio and asymmetries. In the SO(10) case the P-odd asymmetry in $\mu^+ \to e^+\gamma$ varies from -100 to 100 % whereas it is $+100\%$ for the SU(5) case. The P-odd asymmetries in $\mu^+ \to e^+e^+e^-$ are simply proportional to the $\mu^+ \to e^+\gamma$ asymmetry in the SO(10) case and can be predicted from it. On the other hand, with the branching ratios and the P-odd asymmetries in the $\mu^+ \to e^+e^+e^-$ process, we can overdetermine the coupling constants in the effective Lagrangian in the SU(5) SUSY GUT if there are no SUSY CP violating phases. We also calculated the T-odd asymmetry in the $\mu^+ \to e^+e^+e^-$ process with the SUSY CP violating phases and compare it with the neutron, electron, and Hg EDMs. In the SU(5) case we can still determine these coupling constants using additional information of the T-odd asymmetry. The T-odd asymmetry can reach 15% within the constraints of the EDMs. In the SO(10) case the T-odd asymmetry is small as a result of the dominance of photon-penguin diagram. These results are summarized in Table I. We stress that although the magnitude of the branching ratio has a large uncertainty due to the unknown parameter λ_τ, asymmetries and the ratio of two branching ratios are independent of this ambiguity. Thus these quantities are useful to distinguish different models.

The experimental prospects for measuring these quantities depend on the branching ratio. For the SO(10) model we expect the $\mu^+ \to e^+\gamma$ branching ratio can be 10^{-12} when the

TABLE I. Summary of the results.

	SU(5) SUSY GUT	SO(10) SUSY GUT
$A(\mu^+\to e^+\gamma)$	$+100\%$	$-100\%-+100\%$
$\frac{B(\mu^+\to e^+e^+e^-)}{B(\mu^+\to e^+\gamma)}$	$0.007-O(1)$	constant (~ 0.0062)
A_{P_1}	$-30\%-+40\%$	$A_{P1}\simeq -\frac{1}{10}A(\mu^+\to e^+\gamma)$
A_{P_2}	$-20\%-+20\%$	$A_{P2}\simeq -\frac{1}{6}A(\mu^+\to e^+\gamma)$
$\lvert A_T\rvert$	$\lesssim 15\%$	$\lesssim 0.01\%$

λ_τ is given by the corresponding KM matrix elements. In such a case the $\mu^+\to e^+\gamma$ asymmetry can be measurable in an experiment with a sensitivity of 10^{-14} level. For the SU(5) model, to get the $\mu^+\to e^+\gamma$ branching ratio of order 10^{-12} and $\mu^+\to e^+e^+e^-$ branching ratio of 10^{-14}, we have to assume λ_τ is larger than several times 10^{-3}. If the branching ratio turns out to be as large, the $\mu^+\to e^+e^+e^-$ experiments with a sensitivity of 10^{-16} level could reveal various asymmetries. Because various asymmetries are defined with respect to muon polarization, experimental searches for $\mu^+\to e^+\gamma$ and $\mu^+\to e^+e^+e^-$ with polarized muons are very important to uncover the nature of the LFV interactions.

ACKNOWLEDGMENTS

The authors would like to thank Y. Kuno and J. Hisano for useful discussion. The work of Y.O. was supported in part by the Grant-in-Aid of the Ministry of Education, Science, Sports and Culture, Government of Japan (Grant No. 09640381), Priority area ''Supersymmetry and Unified Theory of Elementary Particles'' (Grant No. 707), and ''Physics of *CP* Violation'' (Grant No. 09246105).

APPENDIX A: BRANCHING RATIO AND ASYMMETRIES

In this appendix, we give kinematic functions which appear in the calculation of branching ratio and asymmetries

$$F_i(x)\equiv 2\int_{1-x}^{x} dx_2\,\alpha_i(x,x_2), \tag{A1}$$

$$G_i(x)\equiv 2\int_{1-x}^{x} dx_2\,\beta_i(x,x_2), \tag{A2}$$

$$H_i(x)\equiv -2\int_{1-x}^{x} dx_2\,\gamma_i(x,x_2), \tag{A3}$$

$$F_1(x)=-\frac{8}{3}(4x-5)(2x-1)^2, \tag{A4}$$

$$F_2(x)=-\frac{2}{3}(2x-1)(8x^2-8x-1), \tag{A5}$$

$$F_3(x)=16\ln\left(\frac{x}{1-x}\right)(2x^2-2x+1)+\frac{32}{3}\frac{(2x-1)(x^2-x+1)}{1-x}, \tag{A6}$$

$$F_4(x)=32(2x-1)^2, \tag{A7}$$

$$F_5(x)=-8(2x-1)(2x-3), \tag{A8}$$

$$G_1(x)=-16(1-x)^2\ln 2(1-x)-\frac{2}{3}(2x-1)\times(8x^2-32x+23), \tag{A9}$$

$$G_2(x)=-16(2x^2-2x-7)\ln 2(1-x)+16(2x^2-2x+1)\ln 2x+\frac{32}{3}\frac{(2x-1)(x^2-13x+13)}{1-x}, \tag{A10}$$

$$H_1(x)=2(6-5x)(1-x)\sqrt{2x-1}-(7x^2-24x+16)\sqrt{1-x}\arccos\left(\frac{2-3x}{x}\right)+16(1-x)^2\arccos\left(\frac{1-x}{x}\right), \tag{A11}$$

$$H_2(x)=-16(6-x)\sqrt{2x-1}-8\frac{5x^2+8x-16}{\sqrt{1-x}}\arccos\left(\frac{2-3x}{x}\right)-128\arccos\left(\frac{1-x}{x}\right), \tag{A12}$$

$$H_3(x)=-\frac{4}{3}\sqrt{2x-1}(17x^2-24x+4)+2\frac{(7x-6)x^2}{\sqrt{1-x}}\arccos\left(\frac{2-3x}{x}\right), \tag{A13}$$

$$H_4(x)=+\frac{2}{3}\sqrt{2x-1}(17x^2-30x+16)-\frac{(7x^2-16x+8)x}{\sqrt{1-x}}\arccos\left(\frac{2-3x}{x}\right), \tag{A14}$$

$$I_i[\delta]=\int_{1/2}^{1-\delta} dx F_i(x), \tag{A15}$$

$$J_i[\delta]=\int_{1/2}^{1-\delta} dx G_i(x)dx, \tag{A16}$$

$$K_i[\delta]=\int_{1/2}^{1-\delta} dx H_i(x)dx, \tag{A17}$$

$$I_1[\delta]=\frac{2}{3}(1+2\delta)(1-2\delta)^3, \tag{A18}$$

$$I_2[\delta]=\frac{1}{3}(1+2\delta-2\delta^2)(1-2\delta)^2, \tag{A19}$$

$$I_3[\delta]=\frac{16}{3}(1-\delta)(2-\delta+2\delta^2)\ln\left(\frac{1-\delta}{\delta}\right) - \frac{8}{9}(1-2\delta)(13-4\delta+4\delta^2), \tag{A20}$$

$$I_4[\delta]=\frac{16}{3}(1-2\delta)^3, \tag{A21}$$

$$I_5[\delta]=\frac{8}{3}(1+\delta)(1-2\delta)^2, \tag{A22}$$

$$J_1[\delta]=-\frac{1}{9}-\frac{2}{3}\delta+6\delta^2+\frac{16}{3}\left(\ln 2\delta-\frac{4}{3}\right)\delta^3-\frac{8}{3}\delta^4, \tag{A23}$$

$$J_2[\delta]=-\frac{16}{3}(2+21\delta+3\delta^2-2\delta^3)\ln 2\delta+\frac{16}{3}(1-\delta) \times(2-\delta+2\delta^2)\ln 2(1-\delta) - \frac{8}{9}(1-2\delta)(49+68\delta+4\delta^2), \tag{A24}$$

$$K_1[\delta]=\frac{4}{315}(8+8\delta-93\delta^2-225\delta^3)\sqrt{1-2\delta} - \frac{2}{3}\delta^{\frac{3}{2}}(1-6\delta-3\delta^2)\arccos\left(\frac{3\delta-1}{1-\delta}\right) - \frac{16}{3}\delta^3\arccos\left(\frac{\delta}{1-\delta}\right), \tag{A25}$$

$$K_2[\delta]=\frac{32}{5}(4+9\delta+\delta^2)\sqrt{1-2\delta} - 16\sqrt{\delta}(3+6\delta-\delta^2)\arccos\left(\frac{3\delta-1}{1-\delta}\right) + 128\delta\arccos\left(\frac{\delta}{1-\delta}\right), \tag{A26}$$

$$K_3[\delta]=\frac{8}{105}\sqrt{1-2\delta}(48-57\delta-68\delta^2+85\delta^3) - 4(1-\delta)^3\sqrt{\delta}\arccos\left(\frac{3\delta-1}{1-\delta}\right), \tag{A27}$$

$$K_4[\delta]=\frac{4}{105}\sqrt{1-2\delta}(64-41\delta+26\delta^2-85\delta^3) - 2(1-\delta-\delta^2+\delta^3)\sqrt{\delta}\arccos\left(\frac{3\delta-1}{1-\delta}\right). \tag{A28}$$

APPENDIX B: LFV EFFECTIVE COUPLING CONSTANTS IN MSSM

1. MSSM Lagrangian

We first fix our notations of the MSSM for the numerical calculation. Using

$$v\equiv\sqrt{2(\langle H_2^0\rangle^2+\langle H_1^0\rangle^2)} \tag{B1}$$

and

$$\tan\beta\equiv\frac{\langle H_2^0\rangle}{\langle H_1^0\rangle} \tag{B2}$$

the charged lepton mass matrix is given:

$$(m_e)_{ij}=-(y_e)_{ij}\frac{v}{\sqrt{2}}\cos\beta. \tag{B3}$$

The neutralino and chargino mass matrices are written as follows:

$$\mathcal{L}_N=-\frac{1}{2}(\overline{\tilde{B}_R}\quad\overline{\tilde{W}_{3_R}}\quad\overline{\tilde{H}_{1R}^{0^c}}\quad\overline{\tilde{H}_{2R}^{0^c}})\mathcal{M}_N\begin{pmatrix}\tilde{B}_L\\ \tilde{W}_{3L}\\ \tilde{H}_{1L}^0\\ \tilde{H}_{2L}^0\end{pmatrix}+\text{H.c.},$$

$$\mathcal{M}_N=\begin{pmatrix} M_1 & 0 & -m_z\sin\theta_W\cos\beta & m_z\sin\theta_W\sin\beta \\ 0 & M_2 & m_z\cos\theta_W\cos\beta & -m_z\cos\theta_W\sin\beta \\ -m_z\sin\theta_W\cos\beta & m_z\cos\theta_W\cos\beta & 0 & -\mu \\ m_z\sin\theta_W\sin\beta & -m_z\cos\theta_W\sin\beta & -\mu & 0 \end{pmatrix}, \tag{B4}$$

$$\mathcal{L}_C=-\begin{pmatrix}\overline{\tilde{W}_R^-} & \overline{\tilde{H}_{2R}^{-c}}\end{pmatrix}\mathcal{M}_C\begin{pmatrix}\tilde{W}_L^- \\ \tilde{H}_{1L}^-\end{pmatrix}+\text{H.c.}, \quad \mathcal{M}_C=\begin{pmatrix} M_2 & \sqrt{2}m_W\cos\beta \\ \sqrt{2}m_W\sin\beta & \mu\end{pmatrix}. \tag{B5}$$

They are diagonalized with unitary matrices as follows:

$$O_N\mathcal{M}_N O_N^T=\text{diag}(m_{\tilde{\chi}_1^0},m_{\tilde{\chi}_2^0},m_{\tilde{\chi}_3^0},m_{\tilde{\chi}_4^0}), \tag{B6}$$

$$O_{NR}\equiv O_N, \tag{B7}$$

$$O_{NL}\equiv O_N^*, \tag{B8}$$

$$O_{CR}\mathcal{M}_C O_{CL}^\dagger=\text{diag}(m_{\tilde{\chi}_1^-},m_{\tilde{\chi}_2^-}). \tag{B9}$$

The slepton mass matrices are written as follows:

$$\mathcal{L}_{\tilde{e}}=-\begin{pmatrix}\tilde{L}^{-\dagger} & \tilde{E}^\dagger\end{pmatrix}m_{\tilde{e}}^2\begin{pmatrix}\tilde{L}^- \\ \tilde{E}\end{pmatrix},$$

$$m_{\tilde{e}}^2=\begin{pmatrix} m_L^2+m_e^\dagger m_e+m_z^2\cos 2\beta\left(-\frac{1}{2}+\sin^2\theta_W\right) & \frac{v}{\sqrt{2}}\cos\beta(m_0A_e+y_e\mu^*\tan\beta)^\dagger \\ \frac{v}{\sqrt{2}}\cos\beta(m_0A_e+y_e\mu^*\tan\beta) & m_E^2+m_em_e^\dagger-m_z^2\cos 2\beta\sin^2\theta_W\end{pmatrix}, \tag{B10}$$

$$\mathcal{L}_{\tilde{\nu}}=-\tilde{L}^{0\dagger}m_{\tilde{\nu}}^2\tilde{L}^0,$$

$$m_{\tilde{\nu}}^2=m_L^2-\frac{1}{2}m_z^2\cos 2\beta. \tag{B11}$$

They are diagonalized with unitary matrices as follows:

$$U_em_{\tilde{e}}^2U_e^\dagger=\text{diag}(m_{\tilde{e}_1}^2,m_{\tilde{e}_2}^2,m_{\tilde{e}_3}^2,m_{\tilde{e}_4}^2,m_{\tilde{e}_5}^2,m_{\tilde{e}_6}^2), \tag{B12}$$

$$U_\nu m_{\tilde{\nu}}^2U_\nu^\dagger=\text{diag}(m_{\tilde{\nu}_1}^2,m_{\tilde{\nu}_2}^2,m_{\tilde{\nu}_3}^2). \tag{B13}$$

The neutralino and chargino vertices for leptons and sleptons are written as follows:

$$\mathcal{L}\equiv\overline{e_i}(N_{iAX}^LP_L+N_{iAX}^RP_R)\tilde{\chi}_A^0\tilde{e}_X + \overline{e_i}(C_{iAX}^LP_L+C_{iAX}^RP_R)\tilde{\chi}_A^-\tilde{\nu}_X+\text{H.c.}, \tag{B14}$$

$$N_{iAX}^L=-g\left\{\sqrt{2}\tan\theta_W(O_{NL})_{A1}^*(U_e)_{Xi+3}^* + \frac{(m_e)_{ij}}{\sqrt{2}m_W\cos\beta}(O_{NL})_{A3}^*(U_e)_{Xj}^*\right\}, \tag{B15}$$

$$N_{iAX}^R=-g\left[-\frac{1}{\sqrt{2}}\{(O_{NR})_{A2}^*+\tan\theta_W(O_{NR})_{A1}^*\}(U_e)_{Xi}^* + \frac{(m_e^\dagger)_{ij}}{\sqrt{2}m_W\cos\beta}(O_{NR})_{A3}^*(U_e)_{Xj+3}^*\right], \tag{B16}$$

$$C_{iAX}^L=g\frac{(m_e)_{ij}}{\sqrt{2}m_W\cos\beta}(O_{CL})_{A2}^*(U_\nu)_{Xj}^*, \tag{B17}$$

$$C_{iAX}^R=-g(O_{CR})_{A1}^*(U_\nu)_{Xi}^*. \tag{B18}$$

2. LFV effective coupling constants

The formulas of effective coupling constants for $\mu\to e\gamma$ and $\mu\to 3e$ processes written in the minimal supersymmetric

standard model (MSSM) variables are given in Ref. [26]. We present these formulas for completeness with taking care of the CP violating phases.

Each coupling constant is divided into a neutralino-charged-slepton-loop contribution and chargino-sneutrino-loop contribution. The four-Fermi coupling constants are given as follows:

$$g_i = g_i^n + g_i^c \ (i=1-6). \tag{B19}$$

The coupling constant g_1 comes only from box diagrams:

$$g_1^n = -\frac{\sqrt{2}}{64\pi^2 G_F}\sum_{A,B=1}^{4}\sum_{X,Y=1}^{6}\left(N_{2AX}^L N_{1AY}^{R*} N_{1BY}^L N_{1BX}^{R*} - 2N_{2AX}^L N_{1AY}^L N_{1BY}^{R*} N_{1BX}^{R*}\right)$$
$$m_{\tilde{\chi}_A^0} m_{\tilde{\chi}_B^0} d_0\left(m_{\tilde{\chi}_A^0}^2, m_{\tilde{\chi}_B^0}^2, m_{\tilde{e}_X}^2, m_{\tilde{e}_Y}^2\right), \tag{B20}$$

$$g_1^c = -\frac{\sqrt{2}}{64\pi^2 G_F}\sum_{A,B=1}^{2}\sum_{X,Y=1}^{3} C_{2AX}^L C_{1AY}^{R*} C_{1BY}^L C_{1BX}^{R*}$$
$$m_{\tilde{\chi}_A^-} m_{\tilde{\chi}_B^-} d_0\left(m_{\tilde{\chi}_A^-}^2, m_{\tilde{\chi}_B^-}^2, m_{\tilde{\nu}_X}^2, m_{\tilde{\nu}_Y}^2\right). \tag{B21}$$

The coupling constant g_3 is divided into three parts. g_{31} is a contribution of box diagrams and g_{32} is that of Z-penguin diagrams. g_{33} is a contribution of off-shell photon-penguin diagrams.

$$g_3 = g_{31} + g_{32} + g_{33}, \tag{B22}$$

$$g_{31}^n = -\frac{\sqrt{2}}{64\pi^2 G_F}\sum_{A,B=1}^{4}\sum_{X,Y=1}^{6}\left\{N_{2AX}^L N_{1AY}^{L*} N_{1BY}^L N_{1BX}^{L*} d_2\left(m_{\tilde{\chi}_A^0}^2, m_{\tilde{\chi}_B^0}^2, m_{\tilde{e}_X}^2, m_{\tilde{e}_Y}^2\right) + \frac{1}{2} N_{2AX}^L N_{1AY}^L N_{1BY}^{L*} N_{1BX}^{L*} m_{\tilde{\chi}_A^0} m_{\tilde{\chi}_B^0} d_0\left(m_{\tilde{\chi}_A^0}^2, m_{\tilde{\chi}_B^0}^2, m_{\tilde{e}_X}^2, m_{\tilde{e}_Y}^2\right)\right\}, \tag{B23}$$

$$g_{32}^n = -\frac{1}{16\pi^2} Z_R^e\left[\sum_{A,B=1}^{4}\sum_{X=1}^{6} N_{2AX}^L N_{1BX}^{L*}\left\{4\left(Y_{\tilde{\chi}_L^0}\right)_{AB} c_2\left(m_{\tilde{e}_X}^2, m_{\tilde{\chi}_A^0}^2, m_{\tilde{\chi}_B^0}^2\right) - 2m_{\tilde{\chi}_A^0} m_{\tilde{\chi}_B^0}\left(Y_{\tilde{\chi}_R^0}\right)_{AB} c_0\left(m_{\tilde{e}_X}^2, m_{\tilde{\chi}_A^0}^2, m_{\tilde{\chi}_B^0}^2\right)\right\} + 2\sum_{A=1}^{4}\sum_{X,Y=1}^{6} N_{2AX}^L N_{1AY}^{L*}\left(X_{\tilde{e}_L}\right)_{XY} c_2\left(m_{\tilde{\chi}_A^0}^2, m_{\tilde{e}_X}^2, m_{\tilde{e}_Y}^2\right)\right], \tag{B24}$$

$$g_{33}^n = -\frac{\sqrt{2}e^2}{1152\pi^2 G_F}\sum_{A=1}^{4}\sum_{X=1}^{6} N_{2AX}^L N_{1AX}^{L*}\frac{1}{m_{\tilde{e}_X}^2} b_0^n\left(\frac{m_{\tilde{\chi}_A^0}^2}{m_{\tilde{e}_X}^2}\right), \tag{B25}$$

$$g_{31}^c = -\frac{\sqrt{2}}{64\pi^2 G_F}\sum_{A,B=1}^{2}\sum_{X,Y=1}^{3} C_{2AX}^L C_{1AY}^{L*} C_{1BY}^L C_{1BX}^{L*} d_2\left(m_{\tilde{\chi}_A^-}^2, m_{\tilde{\chi}_B^-}^2, m_{\tilde{\nu}_X}^2, m_{\tilde{\nu}_Y}^2\right), \tag{B26}$$

$$g_{32}^c = -\frac{1}{16\pi^2} Z_R^e\sum_{A,B=1}^{2}\sum_{X=1}^{3} C_{2AX}^L C_{1BX}^{L*}\left\{4\left(Y_{\tilde{\chi}_L^-}\right)_{AB} c_2\left(m_{\tilde{\nu}_X}^2, m_{\tilde{\chi}_A^-}^2, m_{\tilde{\chi}_B^-}^2\right) - 2m_{\tilde{\chi}_A^-} m_{\tilde{\chi}_B^-}\left(Y_{\tilde{\chi}_R^-}\right)_{AB} c_0\left(m_{\tilde{\nu}_X}^2, m_{\tilde{\chi}_A^-}^2, m_{\tilde{\chi}_B^-}^2\right)\right\}, \tag{B27}$$

$$g_{33}^c = -\frac{\sqrt{2}e^2}{1152\pi^2 G_F}\sum_{A=1}^{2}\sum_{X=1}^{3} C_{2AX}^L C_{1AX}^{L*}\frac{1}{m_{\tilde{\nu}_X}^2} b_0^c\left(\frac{m_{\tilde{\chi}_A^-}^2}{m_{\tilde{\nu}_X}^2}\right). \tag{B28}$$

The coupling constant g_5 is divided into three parts. g_{51} is a contribution of box diagrams and g_{52} is that of Z-penguin diagrams. g_{53} is a contribution of off-shell photon-penguin diagrams.

$$g_5 = g_{51} + g_{52} + g_{53}, \tag{B29}$$

$$g_{51}^{n}=-\frac{\sqrt{2}}{64\pi^2 G_F}\sum_{A,B=1}^{4}\sum_{X,Y=1}^{6}\Big\{(N_{2AX}^{L}N_{1AY}^{L*}N_{1BY}^{R}N_{1BX}^{R*}-N_{2AX}^{L}N_{1AY}^{R}N_{1BY}^{R*}N_{1BX}^{L*}$$

$$+N_{2AX}^{L}N_{1AY}^{R}N_{1BY}^{L*}N_{1BX}^{R*})d_2(m_{\tilde{\chi}_A^0}^2,m_{\tilde{\chi}_B^0}^2,m_{\tilde{e}_X}^2,m_{\tilde{e}_Y}^2)-\frac{1}{2}m_{\tilde{\chi}_A^0}m_{\tilde{\chi}_B^0}N_{2AX}^{L}N_{1AY}^{R*}N_{1BY}^{R}N_{1BX}^{L*}d_0(m_{\tilde{\chi}_A^0}^2,m_{\tilde{\chi}_B^0}^2,m_{\tilde{e}_X}^2,m_{\tilde{e}_Y}^2)\Big\}, \tag{B30}$$

$$g_{52}^{n}=-\frac{1}{16\pi^2}Z_L^e\Bigg[\sum_{A,B=1}^{4}\sum_{X=1}^{6}N_{2AX}^{L}N_{1BX}^{L*}\{4(Y_{\tilde{\chi}_L^0})_{AB}c_2(m_{\tilde{e}_X}^2,m_{\tilde{\chi}_A^0}^2,m_{\tilde{\chi}_B^0}^2)-2m_{\tilde{\chi}_A^0}m_{\tilde{\chi}_B^0}(Y_{\tilde{\chi}_R^0})_{AB}c_0(m_{\tilde{e}_X}^2,m_{\tilde{\chi}_A^0}^2,m_{\tilde{\chi}_B^0}^2)\}$$

$$+2\sum_{A=1}^{4}\sum_{X,Y=1}^{6}N_{2AX}^{L}N_{1AY}^{L*}(X_{\tilde{e}_L})_{XY}c_2(m_{\tilde{\chi}_A^0}^2,m_{\tilde{e}_X}^2,m_{\tilde{e}_Y}^2)\Bigg], \tag{B31}$$

$$g_{53}^{n}=g_{33}^{n}, \tag{B32}$$

$$g_{51}^{c}=-\frac{\sqrt{2}}{64\pi^2 G_F}\sum_{A,B=1}^{2}\sum_{X,Y=1}^{3}\Big\{C_{2AX}^{L}C_{1AY}^{L*}C_{1BY}^{R}C_{1BX}^{R*}d_2(m_{\tilde{\chi}_A^-}^2,m_{\tilde{\chi}_B^-}^2,m_{\tilde{\nu}_X}^2,m_{\tilde{\nu}_Y}^2)$$

$$-\frac{1}{2}C_{2AX}^{L}C_{1AY}^{R*}C_{1BY}^{R}C_{1BX}^{L*}m_{\tilde{\chi}_A^-}m_{\tilde{\chi}_B^-}d_0(m_{\tilde{\chi}_A^-}^2,m_{\tilde{\chi}_B^-}^2,m_{\tilde{\nu}_X}^2,m_{\tilde{\nu}_Y}^2)\Big\}, \tag{B33}$$

$$g_{52}^{c}=-\frac{1}{16\pi^2}Z_L^e\sum_{A,B=1}^{2}\sum_{X=1}^{3}C_{2AX}^{L}C_{1BX}^{L*}\{4(Y_{\tilde{\chi}_L^-})_{AB}c_2(m_{\tilde{\nu}_X}^2,m_{\tilde{\chi}_A^-}^2,m_{\tilde{\chi}_B^-}^2)-2m_{\tilde{\chi}_A^-}m_{\tilde{\chi}_B^-}(Y_{\tilde{\chi}_R^-})_{AB}c_0(m_{\tilde{\nu}_X}^2,m_{\tilde{\chi}_A^-}^2,m_{\tilde{\chi}_B^-}^2)\}, \tag{B34}$$

$$g_{53}^{c}=g_{33}^{c}. \tag{B35}$$

Various mixing matrices and Z coupling constants which appear in the above formulas are given as follows:

$$(Y_{\tilde{\chi}_L^0})_{AB}=-\frac{1}{2}\{(O_{NL})_{A3}(O_{NL})_{B3}^{*}-(O_{NL})_{A4}(O_{NL})_{B4}^{*}\}, \tag{B36}$$

$$(Y_{\tilde{\chi}_R^0})_{AB}=\frac{1}{2}\{(O_{NR})_{A3}(O_{NR})_{B3}^{*}-(O_{NR})_{A4}(O_{NR})_{B4}^{*}\}, \tag{B37}$$

$$(Y_{\tilde{\chi}_L^-})_{AB}=-\frac{1}{2}(O_{CL})_{A2}(O_{CL})_{B2}^{*}, \tag{B38}$$

$$(Y_{\tilde{\chi}_R^-})_{AB}=-\frac{1}{2}(O_{CR})_{A2}(O_{CR})_{B2}^{*}, \tag{B39}$$

$$(X_{\tilde{e}_L})_{XY}=-\sum_{k=1}^{3}(U_e)_{Xk}(U_e)_{Yk}^{*}, \tag{B40}$$

$$(X_{\tilde{e}_R})_{XY}=\sum_{k=1}^{3}(U_e)_{Xk+3}(U_e)_{Yk+3}^{*}, \tag{B41}$$

$$Z_L^e=\left(-\frac{1}{2}+\sin^2\theta_W\right), \tag{B42}$$

$$Z_R^e=\sin^2\theta_W. \tag{B43}$$

The photon-penguin coupling constant is written as follows:

$$A_R=A_R^n+A_R^c, \tag{B44}$$

$$A_R^n=\frac{\sqrt{2}e}{256\pi^2 G_F}\sum_{A=1}^{4}\sum_{X=1}^{6}\frac{1}{m^2_{\tilde{e}_X}}\left\{\frac{1}{6}N^R_{2AX}N^{R*}_{1AX}b_1^n\left(\frac{m^2_{\tilde{\chi}^0_A}}{m^2_{\tilde{e}_X}}\right)+N^L_{2AX}N^{R*}_{1AX}\frac{m_{\tilde{\chi}^0_A}}{m_\mu}b_2^n\left(\frac{m^2_{\tilde{\chi}^0_A}}{m^2_{\tilde{e}_X}}\right)\right\}, \tag{B45}$$

$$A_R^c=-\frac{\sqrt{2}e}{128\pi^2 G_F}\sum_{A=1}^{2}\sum_{X=1}^{3}\frac{1}{m^2_{\tilde{\nu}_X}}\left\{\frac{1}{6}C^R_{2AX}C^{R*}_{1AX}b_1^c\left(\frac{m^2_{\tilde{\chi}^-_A}}{m^2_{\tilde{\nu}_X}}\right)+C^L_{2AX}C^{R*}_{1AX}\frac{m_{\tilde{\chi}^-_A}}{m_\mu}b_2^c\left(\frac{m^2_{\tilde{\chi}^-_A}}{m^2_{\tilde{\nu}_X}}\right)\right\}. \tag{B46}$$

The other coupling constants can be obtained by simply exchanging the suffix of above formulas:

$$g_2=g_1(L\leftrightarrow R), \tag{B47}$$

$$g_4=g_3(L\leftrightarrow R), \tag{B48}$$

$$g_6=g_5(L\leftrightarrow R), \tag{B49}$$

$$A_L=A_R(L\leftrightarrow R). \tag{B50}$$

3. Mass functions

The mass functions used in the effective coupling constants of the $\mu^+\to e^+\gamma$ and $\mu^+\to e^+e^+e^-$ processes are defined as follows:

$$b_0^n(x)=\frac{1}{2(1-x)^4}[2-9x+18x^2-11x^3+6x^3\ln(x)], \tag{B51}$$

$$b_1^n(x)=\frac{1}{(1-x)^4}[1-6x+3x^2+2x^3-6x^2\ln(x)], \tag{B52}$$

$$b_2^n(x)=\frac{1}{(1-x)^3}[1-x^2+2x\ln(x)], \tag{B53}$$

$$b_0^c(x)=\frac{1}{2(1-x)^4}[-16+45x-36x^2+7x^3+6(3x-2)\ln(x)], \tag{B54}$$

$$b_1^c(x)=\frac{1}{2(1-x)^4}[2+3x-6x^2+x^3+6x\ln(x)], \tag{B55}$$

$$b_2^c(x)=\frac{1}{2(1-x)^3}[-3+4x-x^2-2\ln(x)], \tag{B56}$$

$$c_0(x,y,z)=-\frac{x\ln(x)}{(y-x)(z-x)}-\frac{y\ln(y)}{(x-y)(z-y)}-\frac{z\ln(z)}{(x-z)(y-z)}, \tag{B57}$$

$$c_2(x,y,z)=\frac{1}{4}\left[\frac{3}{2}-\frac{x^2\ln(x)}{(y-x)(z-x)}-\frac{y^2\ln(y)}{(x-y)(z-y)}-\frac{z^2\ln(z)}{(x-z)(y-z)}\right], \tag{B58}$$

$$d_0(x,y,z,w)=\frac{x\ln(x)}{(y-x)(z-x)(w-x)}+\frac{y\ln(y)}{(x-y)(z-y)(w-y)}+\frac{z\ln(z)}{(x-z)(y-z)(w-z)}+\frac{w\ln(w)}{(x-w)(y-w)(z-w)}, \tag{B59}$$

$$d_2(x,y,z,w)=\frac{1}{4}\left\{\frac{x^2\ln(x)}{(y-x)(z-x)(w-x)}+\frac{y^2\ln(y)}{(x-y)(z-y)(w-y)}+\frac{z^2\ln(z)}{(x-z)(y-z)(w-z)}+\frac{w^2\ln(w)}{(x-w)(y-w)(z-w)}\right\}. \tag{B60}$$

APPENDIX C: APPROXIMATE EXPRESSIONS OF THE PHOTON-PENGUIN AMPLITUDES FOR THE SO(10) MODEL

In this Appendix we discuss the $\mu^+\to e^+\gamma$ amplitude for SO(10) GUT using approximate formulas. Although we used full formulas for numerical analysis, more transparent expressions are obtained in a special parameter region.

The expressions for A_R and A_L are simplified if we use the following approximations.

(1) Keep only dominant contributions. These are parts of terms proportional to m_τ in the neutralino and charged-slepton loop diagrams for both A_R and A_L. For A_R, a part of the chargino-sneutrino loop contribution can also give a large contribution.

(2) Use the fact that, except for the left-right slepton mixings, the slepton mass matrix is almost diagonalized in the

basis where y_u is diagonal and the diagonal elements for the first-two-generations are almost the same. The third generation sleptons become lighter beccause of the effect of the GUT interaction. We treat diagonal elements for the first two generations in the slepton mass matrix exactly degenerate in the approximate formulas and the difference between the third and the first components are denoted as $\Delta m^2_{\tilde{e}_R}$, $\Delta m^2_{\tilde{e}_L}$, and $\Delta m^2_{\tilde{\nu}_L}$, respectively. Neglecting the renormalization effects between the GUT and electroweak scales by small lepton Yukawa coupling constants, these difference are given by Eq. (46). We take into account the left-right mixing of the slepton mass matrix as perturbation.

(3) Take the limit $m_{\tilde{e}_L} \simeq m_{\tilde{e}_R} \simeq m_{\tilde{\nu}_L} = \overline{m} \gg M_{\tilde{\chi}^-_A}, M_{\tilde{\chi}^0_A}$, namely the average slepton mass is much larger than the chargino and neutralino masses.

Within these approximations A_R and A_L are given by

$$A_R \simeq -\frac{e\tan^2\theta_W}{32\pi^2}[e^{-i(\phi_2-\phi_3)}a^n + a^c], \tag{C1}$$

$$A_L \simeq -\frac{e\tan^2\theta_W}{32\pi^2}[e^{-i(\phi_3-\phi_1)}a^{n*}], \tag{C2}$$

where

$$a^n = (V^0_{KM})_{32}(V^0_{KM})^{*2}_{33}(V^0_{KM})_{31}\left(\frac{m_\tau}{m_\mu}\right)\frac{\left(m_0\frac{A_{e3}}{y_\tau}+\mu^*\tan\beta\right)}{\overline{m}}\left(\frac{m_W}{\overline{m}}\right)^2\left(\frac{M_1}{\overline{m}}\right)\left(\frac{\Delta m^2_{\tilde{e}_L}}{\overline{m^2}}\right)\left(\frac{\Delta m^2_{\tilde{e}_R}}{\overline{m^2}}\right), \tag{C3}$$

$$a^c = (V^0_{KM})^*_{32}(V^0_{KM})_{31}\frac{\sqrt{2}\cot^2\theta_W}{\cos\beta}\sum_{A=1}^{2}(O_{CL})^*_{A2}(O_{CL})_{A1}\frac{m_W}{\overline{m}}\ln\left(\frac{\overline{m^2}}{M^2_{\tilde{\chi}^-_A}}\right)\left(\frac{M_{\tilde{\chi}^-_A}}{\overline{m}}\right)\left(\frac{\Delta m^2_{\tilde{\nu}_L}}{\overline{m^2}}\right). \tag{C4}$$

For the neutralino contributions, difference between the above expression and the exact calculation is within 10 % above $m_{\tilde{e}_R} > 500$ GeV for the parameter set of Fig. 7. For chargino contributions the approximation is slightly worse. At $m_{\tilde{e}_R} > 500$ GeV the difference is within a factor of 2 and becomes about 10% level for $m_{\tilde{e}_R} = 1000$ GeV. From the above expression we can see that despite lack of the factor m_τ/m_μ the chargino contribution can become comparable to or even dominant over the neutralino contribution when $\overline{m} \gg m_W$ because of the enhancement factors $\sqrt{2}\cot^2\theta_W/\cos\beta$ and $(\overline{m}/m_W)\ln(\overline{m^2}/M^2_{\tilde{\chi}^-_A})$.

APPENDIX D: NEUTRON EDM

We discuss QCD correction in the calculation of the neutron EDM [21,27]. The neutron EDM are calculated by the following effective Lagrangian:

$$\mathcal{L}_{\rm eff} = \sum_q C^E_q(\mu)\mathcal{O}^E_q(\mu) + \sum_q C^C_q(\mu)\mathcal{O}^C_q(\mu) + C^G(\mu)\mathcal{O}^G(\mu), \tag{D1}$$

where $\mathcal{O}^E_q$, $\mathcal{O}^C_q$, $\mathcal{O}^G$ correspond to the quark electric dipole, chromomagnetic dipole, and gluonic Weinberg's operators, respectively, which are given by

$$\mathcal{O}^E_q = -\frac{i}{2}\overline{q}\sigma_{\mu\nu}\gamma_5 q F^{\mu\nu}, \tag{D2}$$

$$\mathcal{O}^C_q = -\frac{i}{2}\overline{q}\sigma_{\mu\nu}\gamma_5 T^a q G^{a\mu\nu}, \tag{D3}$$

$$\mathcal{O}^G = -\frac{1}{6}f^{abc}\epsilon^{\mu\nu\lambda\rho}G^a_{\lambda\rho}G^b_{\mu\alpha}G^{c\alpha}_{\nu}. \tag{D4}$$

Here, $\epsilon^{0123}=1$, and f^{abc} is the structure constant of the SU(3) group.

In SUSY models, we can obtain the Wilson coefficients at the electroweak scale by evaluating one-loop diagrams. C^E_q is induced by the photon-penguin diagram. C^c_q is induced by the gluon-penguin diagram. There are three types of SUSY contribution, chargino-squark loop, neutralino-squark loop, and gluino-squark loop diagrams. The gluonic Weinberg's operator is induced at a two-loop level and the diagram involving the stop and the gluino gives dominant contribution. These contributions are listed in Ref. [21].

We can take into account a QCD correction from the electroweak scale to a hadronic scale (1 GeV), by using the following renormalization group equations for the Wilson coefficients:

$$\mu\frac{d\vec{C}(\mu)}{d\mu} = \frac{\alpha_s(\mu)}{4\pi}\gamma^T\vec{C}(\mu), \tag{D5}$$

where $\vec{C} = (C^E_q, C^C_q, C^G)^T$ and the anomalous dimension matrix γ_{ij} is written by

$$\gamma=\begin{pmatrix} 8/3 & 0 & 0 \\ 32eQ/(3g_s) & (-29+2N_f)/3 & 0 \\ 0 & 6m_q & 2N_f+3 \end{pmatrix}. \tag{D6}$$

Here, N_f is a number of the quark flavor and Q denotes the electromagnetic charge of the quark in unit e ($e>0$). The RGEs can be solved analytically as follows:

$$C_q^E(\mu)=\eta^{8/(33-2N_f)}\Bigg[C_q^E(\mu_0) + 8eQ(1-\eta^{-4/(33-2N_f)})\frac{C_q^C(\mu_0)}{g_s(\mu_0)}-\frac{72eQm_q(\mu_0)}{7+2N_f} \times\Bigg(1-\eta^{-4/(33-2N_f)}+\frac{2}{2N_f+5} \times(1-\eta^{(10+4N_f)/(33-2N_f)})\Bigg)\frac{C_G(\mu_0)}{g_s(\mu_0)}\Bigg], \tag{D7}$$

$$C_q^C(\mu)=\eta^{(-29+2N_f)/(33-2N_f)}\Bigg[C_q^C(\mu_0) - \frac{9}{7+2N_f}(1-\eta^{(14+4N_f)/(33-2N_f)}) \times m_q(\mu_0)C^G(\mu_0)\Bigg], \tag{D8}$$

$$C^G(\mu)=\eta^{(9+6N_f)/(33-2N_f)}C^G(\mu_0), \tag{D9}$$

where $\eta=g_s(\mu_0)/g_s(\mu)$.

We solve RGE from m_W to m_b, m_b to m_c, and m_c to the 1 GeV scale. When the heavy quarks (c,b) decouple at their mass threshold, C^G is induced through the chromoelectric dipole moment of the heavy quarks. Difference C^G below and above the threshold is given by [28]

$$C^G(m_q)_{\text{below}}-C^G(m_q)_{\text{above}}=+\frac{\alpha_s(m_q)}{8\pi m_q(m_q)}C_q^C(m_q). \tag{D10}$$

Taking into account the QCD and threshold corrections, we obtain the effective Lagrangian at the hadronic scale. It is then straightforward to evaluate the effective $\mathcal{L}$ at 1 GeV scale from m_W scale.

The neutron EDM (d_n) is given by the Wilson coefficients at a hadronic scale as follows:

$$d_n=d_n^E+d_n^C+d_n^G, \tag{D11}$$

$$d_n^E=\frac{1}{3}(4C_d^E-C_u^E), \tag{D12}$$

$$d_n^C=\frac{1}{3}\frac{e}{4\pi}(4C_d^C-C_u^C), \tag{D13}$$

$$d_n^G=\frac{eM}{4\pi}C^G, \tag{D14}$$

where M is a chiral symmetry breaking parameter, which is estimated as 1.19 GeV. In the above we use nonrelativistic quark model for d_n^E and naive dimensional analysis for d_n^C and d_n^G.

[1] R. Barbieri and L. J. Hall, Phys. Lett. B **338**, 212 (1994).

[2] R. Barbieri, L. Hall, and A. Strumia, Nucl. Phys. **B445**, 219 (1995); **B449**, 437 (1995).

[3] J. Hisano, T. Moroi, K. Tobe, and M. Yamaguchi, Phys. Lett. B **391**, 341 (1997); **397**, 357(E) (1997).

[4] N. Arkani-Hamed, H. Cheng, and L. J. Hall, Phys. Rev. D **53**, 413 (1996); P. Ciafaloni, A. Romanino, and A. Strumia, Nucl. Phys. **B458**, 3 (1996); T. V. Duong, B. Dutta, and E. Keith, Phys. Lett. B **378**, 128 (1996); M. E. Gomez and H. Goldberg, Phys. Rev. D **53**, 5244 (1996); N. G. Deshpande, B. Dutta, and E. Keith, *ibid.* **54**, 730 (1996); S. F. King and M. Oliveira, *ibid.* **60**, 035003 (1999).

[5] M. L. Brooks *et al.*, Phys. Rev. Lett. **83**, 1521 (1999).

[6] SINDRUM Collaboration, U. Bellgradt *et al.*, Nucl. Phys. **B299**, 1 (1988).

[7] SINDRUM II Collaboration, talk given at the International Conference on High Energy Physics, Vancouver, July, 1998 (unpublished).

[8] L. M. Barkov *et al.*, ''Search for the decay $\mu^+\to e^+\gamma$ down to 10^{-14} branching ratio,'' research proposal to Paul Scherrer Institut, 1999 (unpublished).

[9] M. Bachman *et al.*, ''A Search for $\mu N\to eN$ with sensitivity below 10^{-16} MECO,'' proposal to Brookhaven National Laboratory AGS, 1997 (unpublished).

[10] A. E. Pifer, T. Bowen, and K. R. Kendall, Nucl. Instrum. Methods **135**, 39 (1976).

[11] Y. Kuno and Y. Okada, Phys. Rev. Lett. **77**, 434 (1996); Y. Kuno, A. Maki, and Y. Okada, Phys. Rev. D **55**, 2517 (1997).

[12] S. B. Treiman, F. Wilczek, and A. Zee, Phys. Rev. D **16**, 152 (1977); A. Zee, Phys. Rev. Lett. **25**, 2382 (1985).

[13] Y. Okada, K. Okumura, and Y. Shimizu, Phys. Rev. D **58**, 051901 (1998).

[14] J. Hisano and D. Nomura, Phys. Rev. D **59**, 116005 (1999).

[15] J. Ellis, S. Ferrara, and D. V. Nanopoulos, Phys. Lett. **114B**, 231 (1982); W. Buchmüller and D. Wyler, *ibid.* **121B**, 393 (1983); J. Polchinski and M. Wise, *ibid.* **125B**, 393 (1983); F. del Aguila, M. Gavela, J. Grifols, and A. Mendez, *ibid.* **126B**, 71 (1983); D. V. Nanopoulos and M. Srednicki, *ibid.* **128B**, 61 (1983); M. Dugan, B. Grinstein, and L. Hall, Nucl. Phys. **B255**, 413 (1985); Y. Kizukuri and N. Oshimo, Phys. Rev. D **45**, 1806 (1992); **46**, 3025 (1992).

[16] T. Falk, K. A. Olive, M. Pospelov, and R. Roiban, Nucl. Phys. **B560**, 3 (1999).

[17] J. Hisano, D. Nomura, Y. Okada, Y. Shimizu, and M. Tanaka, Phys. Rev. D **58**, 116010 (1998).

[18] S. Dimopoulos and L. J. Hall, Phys. Lett. B **344**, 185 (1995).

[19] T. Goto, Y. Okada, and Y. Shimizu, Phys. Rev. D **58**, 094006 (1998).
[20] CLEO Collaboration, Report No. CONF 98-17, ICHEP98 1011.
[21] T. Ibrahim and P. Nath, Phys. Lett. B **418**, 98 (1998); Phys. Rev. D **57**, 478 (1998); **58**, 111301 (1998).
[22] E. D. Commins, S. B. Ross, D. DeMille, and B. C. Regan, Phys. Rev. A **50**, 2960 (1994).
[23] P. G. Harris, C. A. Baker, K. Green, P. Iaydjiev, and S. Ivanov, Phys. Rev. Lett. **82**, 904 (1999).
[24] J. P. Jacobs *et al.*, Phys. Rev. Lett. **71**, 3782 (1993).
[25] T. Falk and A. Olive, Phys. Lett. B **375**, 196 (1996).
[26] J. Hisano, T. Moroi, K. Tobe, and M. Yamaguchi, Phys. Rev. D **53**, 2442 (1996).
[27] E. Braaten, C. S. Li, and T. C. Yuan, Phys. Rev. Lett. **64**, 1709 (1990); R. Arnowitt, J. L. Lopez, and D. V. Nanopoulos, Phys. Rev. D **42**, 2423 (1990).
[28] D. Chang, W. Y. Keung, C. S. Li, and T. C. Yuan, Phys. Lett. B **241**, 589 (1990).